FOURTH INTERIM DEVELOPMENT REPORT

FOR

DEVELOPMENT OF A FERRITE MATERIAL

FOR A HIGH POWER PHASE SHIFTER

AT S-BAND

This report covers the period 18 January 1963 to 18 April 1963

AIRTRON, A DIVISION OF LITTON INDUSTRIES

200 EAST HANOVER AVENUE

MORRIS PLAINS, NEW JERSEY

NAVY DEPARTMENT BUREAU OF SHIPS ELECTRONICS DIVISION

NOBSR 87388

May 20, 1963

TABLE OF CONTENTS

Table of Contents (continued)

LIST OF ILLUSTRATIONS

List of Illustrations (continued)

List of Illustrations (continued)

1. ABSTRACT

Numerous batches of composition 4 initially were prepared using conventional ceramic methods. The amount of milling, calcining temperature, and firing cycle were varied. Samples from these various treatments were thoroughly evaluated.

Several batches of composition 4 were flame sprayed. Fifteen flame sprayed samples were hot pressed in the small hot press. Hot pressing, number 28, yielded a material with loss properties similar to TT-414. This was the "ultra" fine material collected in the water. It is felt that of all the flame sprayed, hot pressed materials this material showed the most promise of meeting the contract specifications.

The new hydraulic system was completed on the large hot press and a 6" x 1" x 1/4" sample was successfully hot pressed.

2. PURPOSE

The purpose of this contract is to develop a ferrite material suitable for operation at 250 Kw peak power in a phase shifter device operating at S-band frequencies. This work will primarily be centered around the nickel aluminum gallium ferrite system. Better insight into the behavior of this system will be obtained by measuring the microwave properties as a function of power level. It is anticipated that a Reggia-Spencer type phase shifter will be constructed utilizing a ferrite in this new system.

3. MATERIAL DEVELOPMENT

3.1 Compositional Study

The measurements that have been made indicate that compositions near NAGS-4 have the best possibility of fulfilling the device requirements. Due to iron pick-up during milling as discussed in Section 3.2, compositions with total trivalent ion content (Table VIII) ranging from 1.963 to 2.076 were produced. The test results indicate a composition close to NAGS-4 but nearer stoichiometry should be prepared.

3.2 Ceramic Processing

In order to determine the effect of ceramic process variations on the physical and electrical properties of composition NAGS-4, the following experiments were undertaken. Twelve batches were prepared. Three of each of these batches were milled for 6, 12, 24, and 48 hours. One batch from each milling time was calcined at 1050°C, 1125°C, and 1200°C; all for 5 hours. The material was then remilled with binders added during the last 4 hours so that the total milling time was 12, 24, 48, and 96 hours. The dried powder was then pressed into bars at 10,000 psi and fired at three temperatures, 1325°C, 1350°C, and 1375°C, all for 10 hours in oxygen. Measurements of density, porosity, 20 Mc tan δ , ΔH, "g", and $4\pi M_s$ were made on all samples. The physical data obtained are given in Table I.

The rate of temperature increase for all firings was kept constant. The cooling rate was controlled to as low a temperature as possible.

TABLE I

PHYSICAL DATA

NAGS Sample	Total Milling Time	Calcine Temp.	% Fe_2O_3 in Formulation	% Fe_2O_3 Analyzed	Firing # 1128 1320°C *		Firing # 1115 1350°C *			Firing # 1149 1375°C *		Firing # 1156 1375°C**
					Por.	$4\pi M_s$	Por.	T_c	$4\pi M_s$	Por.	$4\pi M_s$	Por.
4E-1	12	1050	35.31	37.02	9.76	631	.20	189	661	.34	722	6.02
4E-2	12	1125	35.31	36.77	8.03	554	.47	195	665	1.17	676	4.52
4E-3	12	1200	35.31	37.47	7.28	651	.25	195	733	1.90	648	4.40
4P-1	24	1050	35.31	37.48	7.44	657	1.27	187	653	.14	715	2.75
4P-2	24	1125	35.31	37.08	2.49	693	0.0	190	772	.92	656	.81
4P-3	24	1200	35.31	37.14	3.91	625	.81	191	712	.49	695	.94
4G-1	48	1050	35.31	38.32	1.25	635	0.16	193	810	.46	728	1.07
4G-2	48	1125	35.31	38.31	3.35	650	2.93	203	604	1.56	621	2.43
4G-3	48	1200	35.31	38.31	1.37	592	0.00	193	770	.25	682	1.12
4H-1	96	1050	35.31	38.52	2.03	582	.2	206	666	.32	657	.84
4H-2	96	1125	35.31	39.30	1.02	590	.2	207	672	.37	659	.75
4H-3	96	1200	35.31	39.35	1.23	611	.6	210	686	.61	685	.82

* 10 hours soak.
** 1 hour soak.

Material Development (continued)

A typical firing cycle is shown in Figure 1.

After the second milling, the batches were analyzed to determine iron pick-up during ball milling. The data obtained are listed in Table I and Table VII. The iron content vs. milling time has been plotted in Figure 2.

The linear shrinkage for the 1350°C firing vs. milling time for each calcining temperature is plotted in Figure 3. This result is typical for all firings.

Plots of porosity vs. firing temperature for each series at a given milling time are shown in Figures 4, 5, 6, and 7.

In order to observe the effect of soak time on the properties of this composition, a firing was made at a peak temperature or 1375°C, held for one hour. The result is a higher porosity with the short soak period.

Two thousand (2,000) grams of NAGS-4 were prepared and calcined at 1100°C for 5 hours. This NAGS-4 material is very similar to 4G2 material. Large bars, 1" x 1" x 6", were pressed and fired at 1350°C for 10 hours in oxygen. This firing was repeated with another bar to check reproducibility. Evaluation of this material has not been made. The bars from the two firings had a crack along the 6 inch dimension. It will be possible to make one bar from the two bars that will have the required dimensions for evaluation in the high power phase shifter.

3.3 Flame Spraying

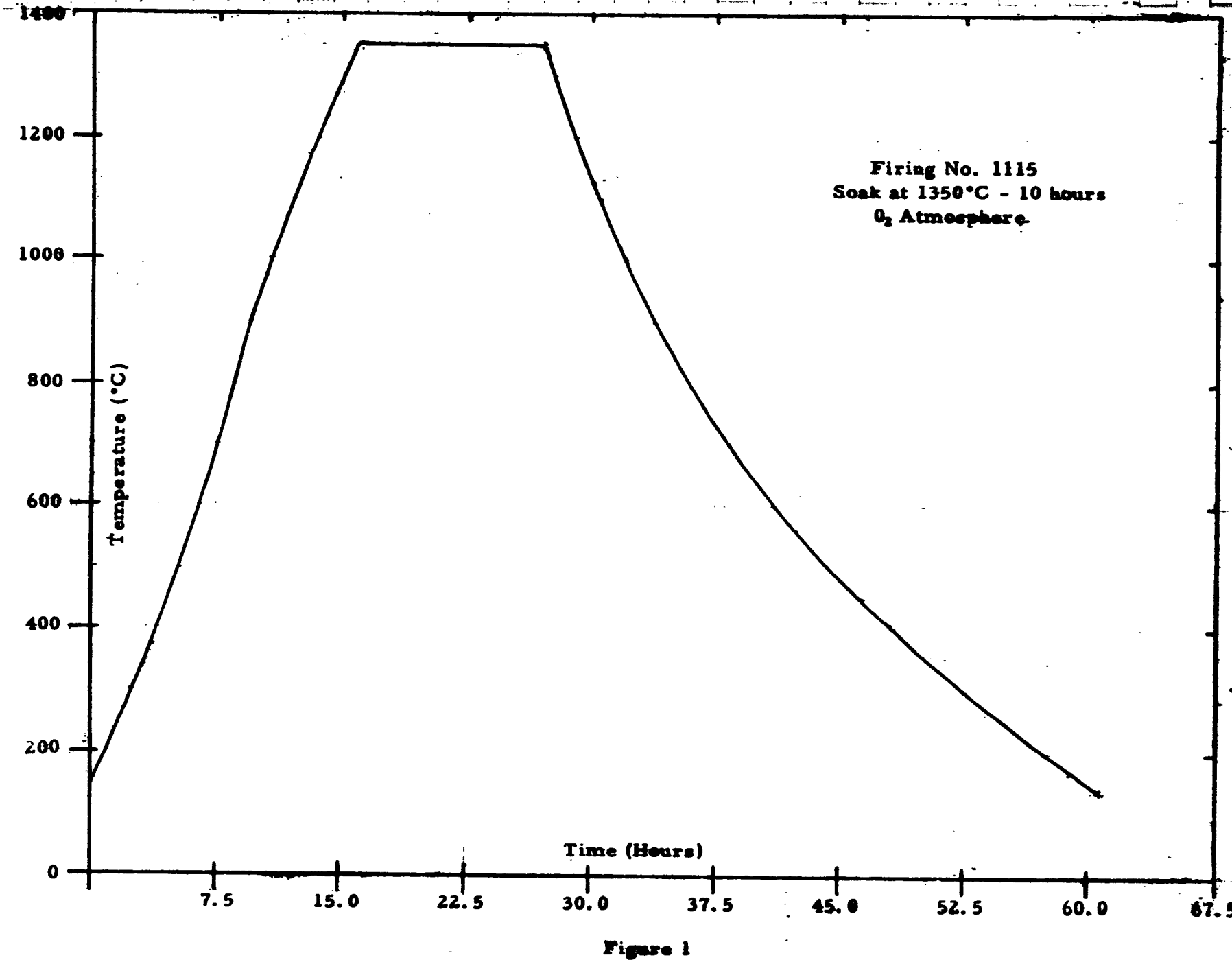
Firing No. 1115
Soak at 1350°C - 10 hours
0_2 Atmosphere
Temperature (°C)
Time (Hours)
1400
1200
1000
800
600
400
200
0
7.5
15.0
22.5
30.0
37.5
45.0
52.5
60.0
67.5

Figure 1

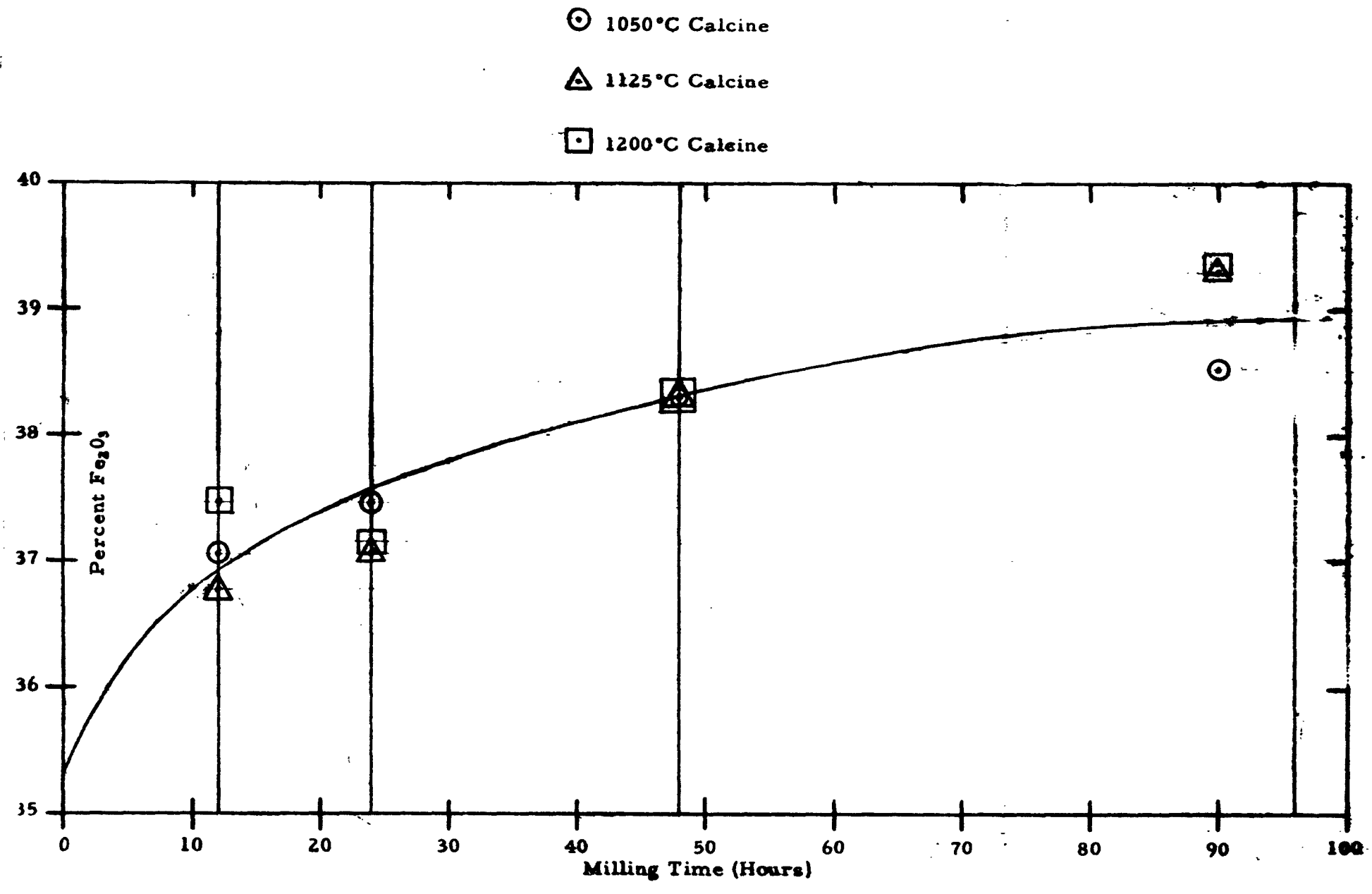

Figure 2
Iron Content vs. Milling Time

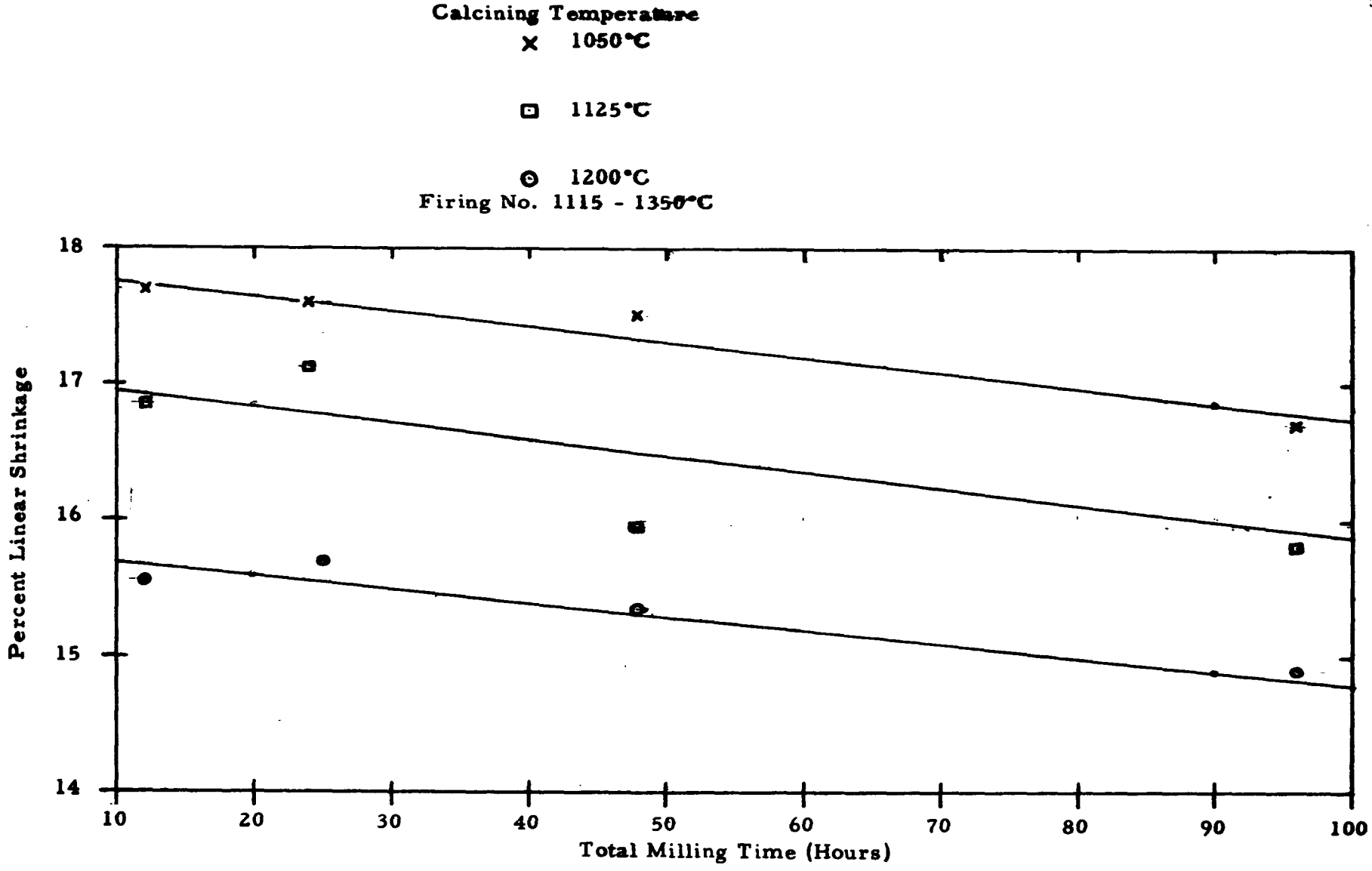

Figure 3
Linear Shrinkage vs. Total Milling Time

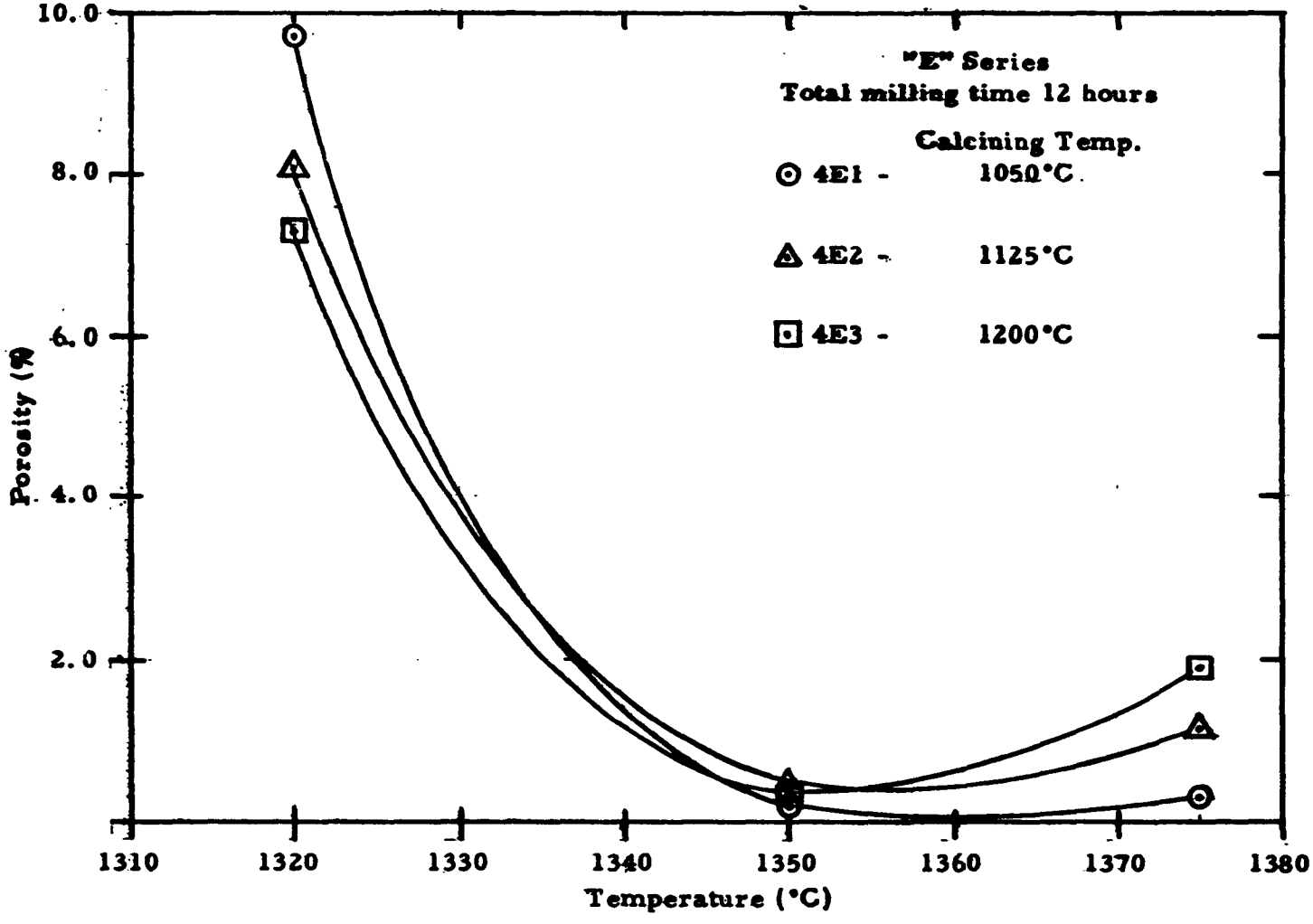

R11-421

Figure 4
Porosity vs. Temperature

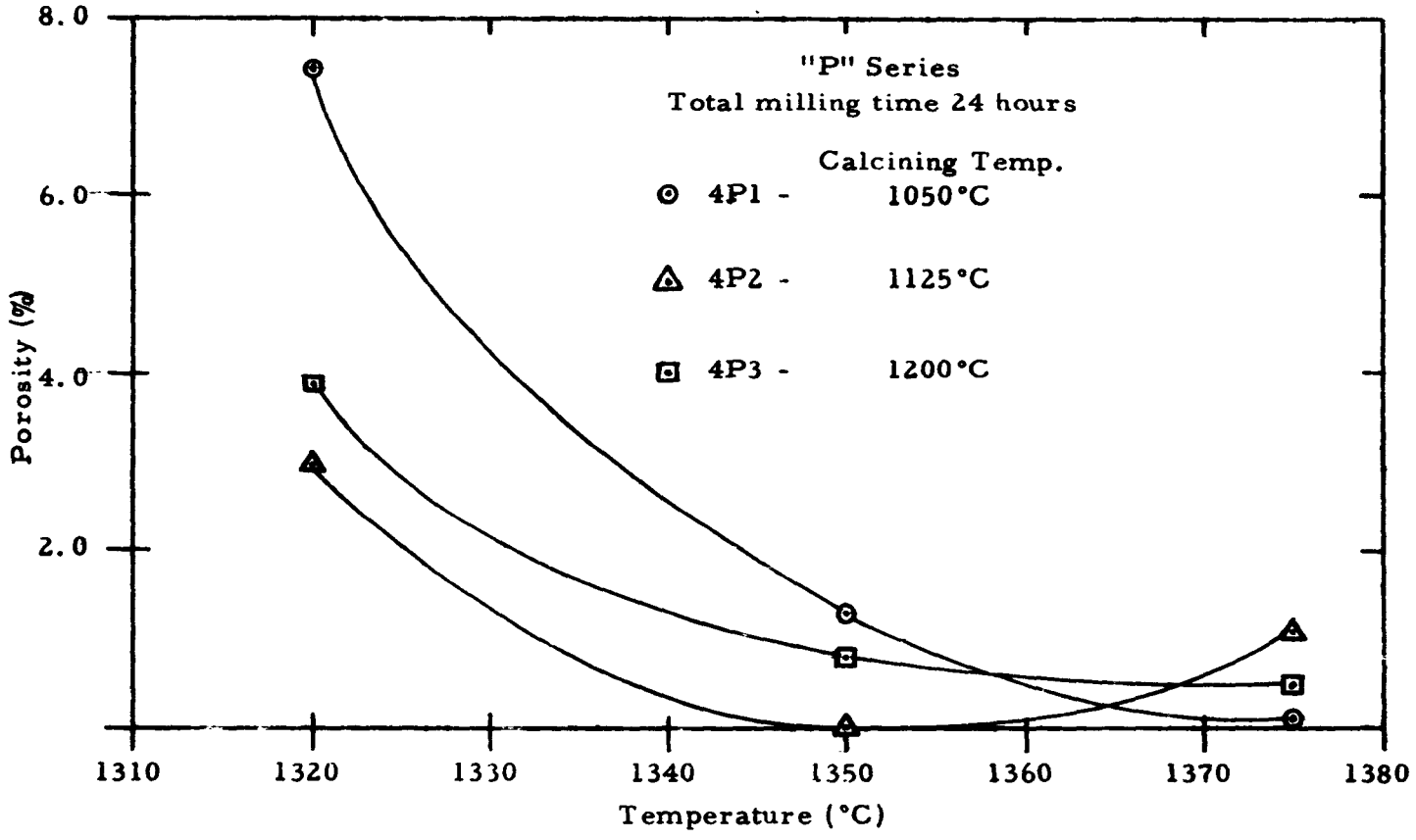

Figure 5
Porosity vs. Temperature

R11-421

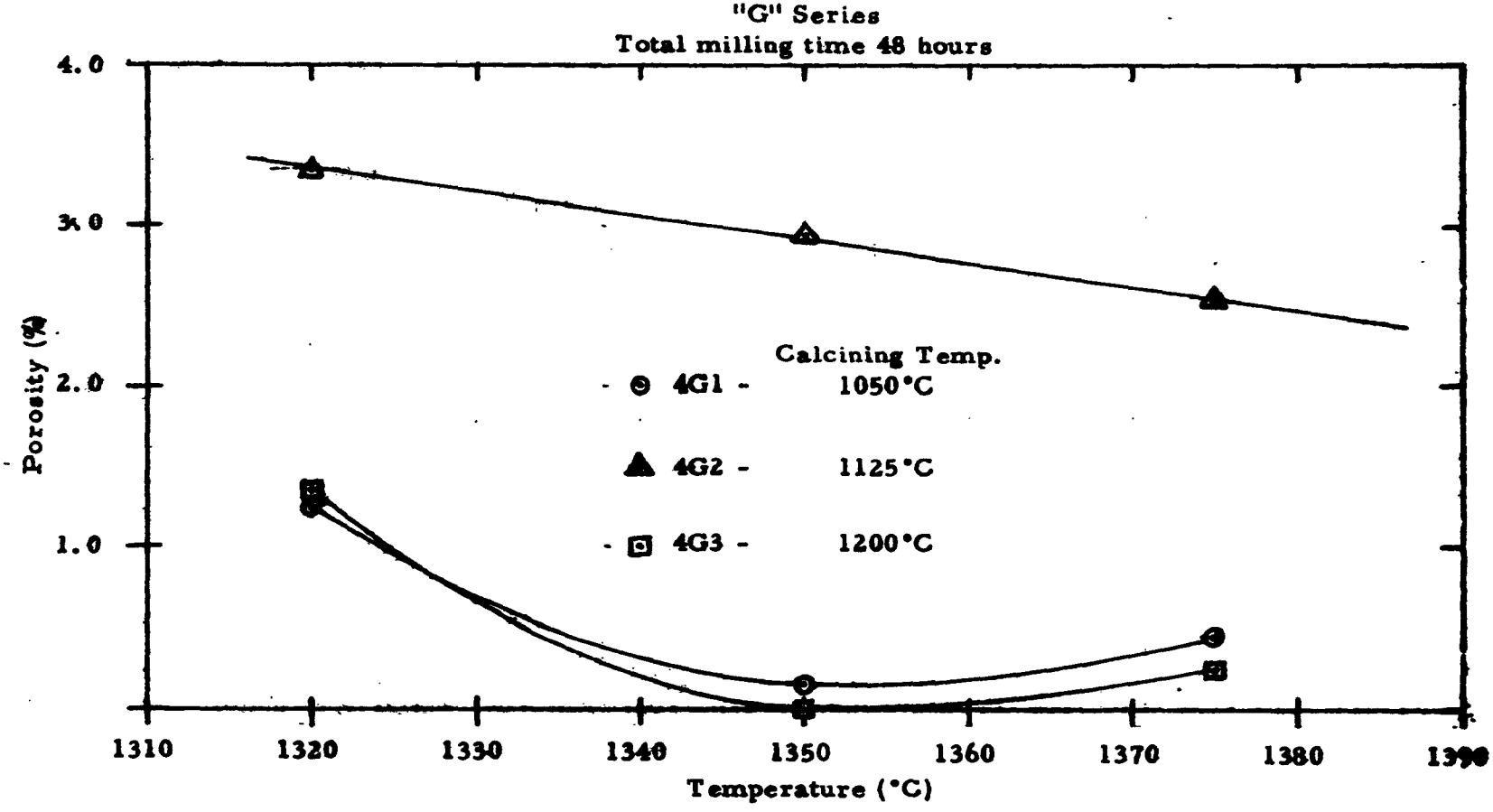

Figure 6
Porosity vs. Temperature

M11-421

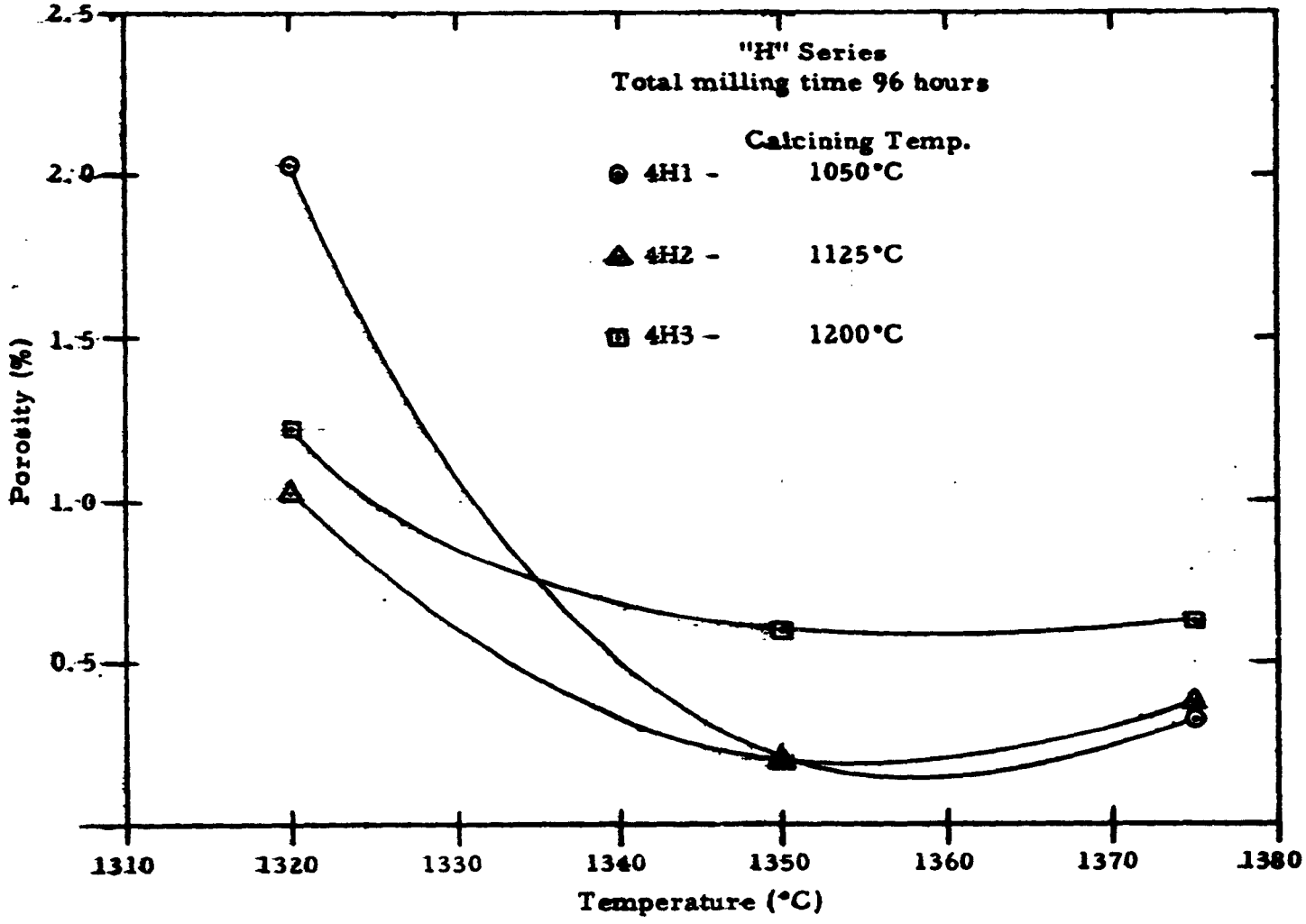

Figure 7
Porosity vs. Temperature

R11-421

Material Development (continued)

3.3.1 Flame Spraying Apparatus

The flame spray apparatus has been modified in order to improve the burning conditions and increase powder yield. Three significant changes have been incorporated.

1. Before modification, secondary air was inspirated into the sidearm in large quantities. The secondary air had two adverse effects: it cooled the combustion flame, and added considerable volume to the flow of gases and powder through the sidearm and into the gas scrubber compartment. A stainless steel plate, with suitable holes for the acetylene torch and nozzle, was fastened to the end of the sidearm, thus reducing the secondary air to a minimum.

2. A removable series of perforated baffles was installed in the sidearm to slow down the velocity of the gases and powder and to increase settling. Also, a perforated metal plate has been placed above the gas scrubber to aid in slowing down the combustion products.

3. A recirculating fine particles collector has been installed and is shown in Figure 8. The water from the scrubber nozzle is fed to the series of overflow settling trays. Permanent magnets are placed beneath the trays to aid the settling. The nearly powder-free water from the final settling tray is pumped back through the scrubber nozzle to complete the cycle. The series of settling trays also enables further particle size separation, heretofore not possible.

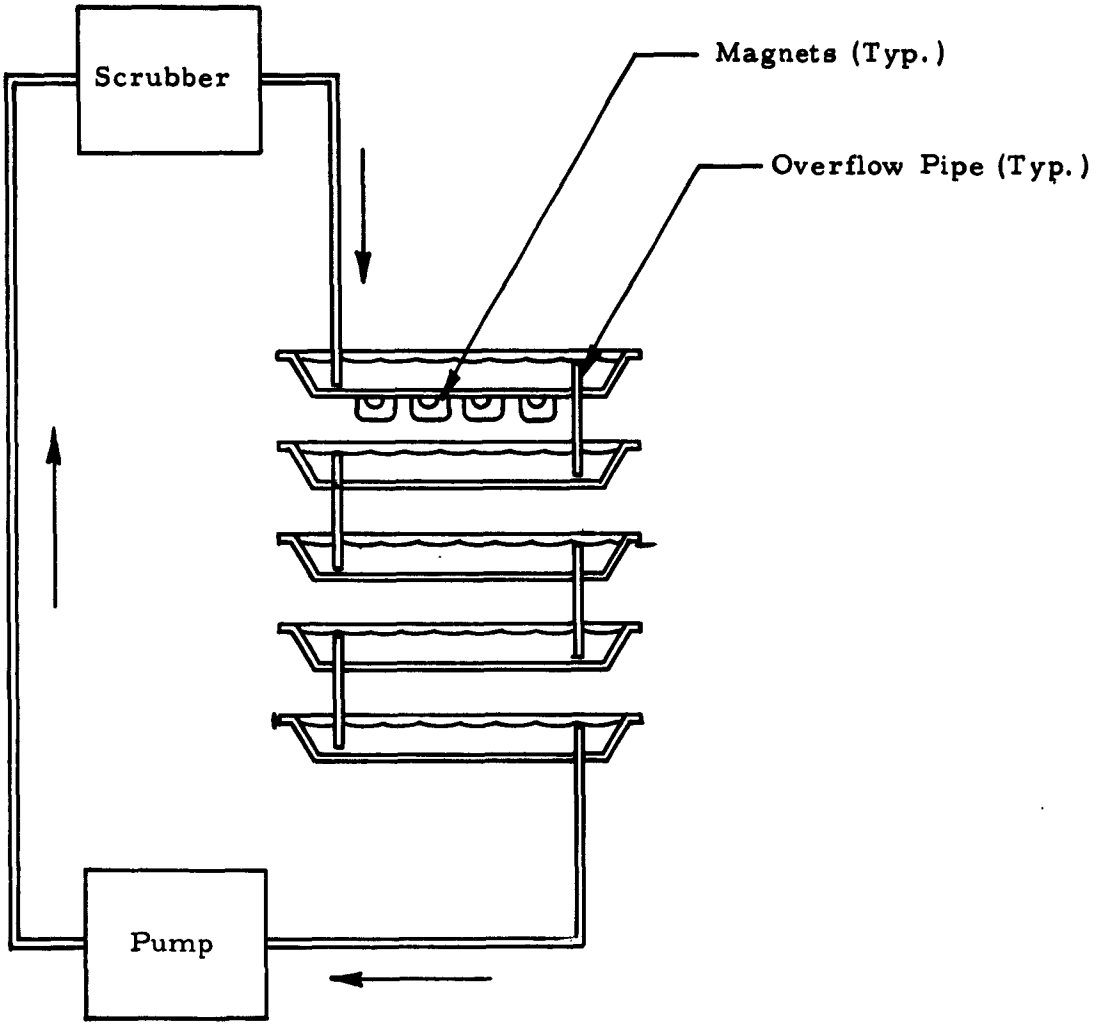

Water in closed circuit from spray nozzle to tanks→pump→spray nozzle

Figure 8
Settling System

Material Development (Continued)

A multi-port, ring-type acetylene air torch is being prepared by the Asco Company. If an operable torch can be fabricated, burning conditions at the nozzle should be improved. A mounting is being fabricated for the nozzle and torches which should aid in reproducing batches.

3.3.2 Flame Spray Batches

NAGS-4-4 and NAGS-4-6 were run after the flame spray apparatus was modified as described in the previous section. The yields are greatly improved and are given in Table II.

Iron analysis from these batches indicate near stoichiometric burning as shown in Table III. The data indicate a small compositional difference between the sidearm material and the fines; however, there is no difference in color, contrary to observations made on earlier runs. The fines have a slightly increased iron content, but the total trivalent metal oxide is less than 2.0 and is, therefore, iron deficient. As a result of the improved burning conditions, the difference between the sidearm and tank materials has been minimized.

Two separate high temperature reactions may create the excess Fe_2O_3 content observed in the fines, see Table III. Should some of the ferric iron be reduced to the ferrous state, analysis of the total amount of iron present with subsequent conversion to Fe_2O_3 would yield a higher Fe_2O_3 percentage than expected. The second effect is that the gallium and aluminum oxides are more readily soluble in the water vapor generated by

TABLE II

FLAME SPRAY YIELD

Batch	Specific Gravity	Theoretical Yield (gms)	Actual Yield Sidearm (gms)	Actual Yield Fines (gms)	%Yield Sidearm	%Yield Fines	Total % Yield
3-4	1.325	465	160	36	34.4	7.8	42.2
4-4	1.320	225	127	16	56.5	7.0	63.5
4-6	1.225	225	139	10	61.7	4.5	66.2
4-7	1.325	1313	801	178	61.0	13.5	74.5
7-1	-----	291	168	15	57.7	5.1	62.8

TABLE III

PERCENT Fe_2O_3

Batch	% Fe_2O_3 Expected	% Fe_2O_3 Sidearm	% Fe_2O_3 Fines
4-4	35.31	35.09	36.78
4-6	35.31	36.18	-----
4-7	35.31	35.06	36.69
7-1	37.70	37.48	-----

Material Development (continued)

combustion and could, therefore, be removed in the exhausting vapor. This theory can be checked by analyzing for NiO, which should also appear higher than the initial batch. Because gallium and aluminum nitrates may thermally decompose to the oxide faster than iron nitrate, iron analyses of the sidearm material may be less than anticipated. This theory can also be checked by analyzing the NiO content; it should be smaller than initially in the sidearm also. These analyses are scheduled for the final quarter.

A large batch of composition 3 (batch 3-4) was flame sprayed with a 42.2 percent yield, see Table II. This composition was prepared using the flame spray technique to compare its properties with those of composition 4.

A large batch of composition 4 was also flame sprayed (batch 4-7) similar to 4-4 and 4-6. NAGS-4-7 had a 74.5 percent yield. Portions of the sidearm (Sa) and fines (Ft) are presently being hot pressed for evaluation. After the proper material composition and pressing cycle necessary to obtain the desired electrical magnetic properties are determined using the small hot press, larger pieces, 1" x 1" x 6", will be processed in the large hot press.

3.4 Hot Pressing

3.4.1 Hot Pressing Apparatus

3.4.1.1 Large Hot Press Die

The large hot press die described in the Third

Material Development (continued)

Interim Development Report has been built and operated successfully. The die is shown in Figure 9.

A 1" x 1" x 1/4 inch bar of flame sprayed C20 (a standard Airtron production material in the NAGS system) has been hot pressed using the large die and is presently being evaluated. The bar was pressed at 1110°C and 4000 psig for 30 minutes. The sample is designated as HP_{x-3}.

The large die weighs in excess of 300 pounds and was extremely difficult to handle. A pulley system has been built which should aid in the loading and unloading operations. Other minor modifications are also being made in order to increase the operating efficiency of the large die.

3.4.1.2 Large Hot Press Hydraulic System

Airtron, in co-ordination with the Air Royal Hydraulic Co., has modified its 400 ton press for hot pressing experiments. The press is now capable of accurately maintaining low pressures for long periods of time. Line pressures as low as 50 psi, which sustains a die operating pressure of 2,000 psi, can be held for 120 minutes. The line pressure drift over this period of time is less than 10 percent and can be periodically adjusted. Higher line pressures and die operating pressures can be maintained more accurately, for example, at 100 psi line pressure, the drift is less than 5 percent.

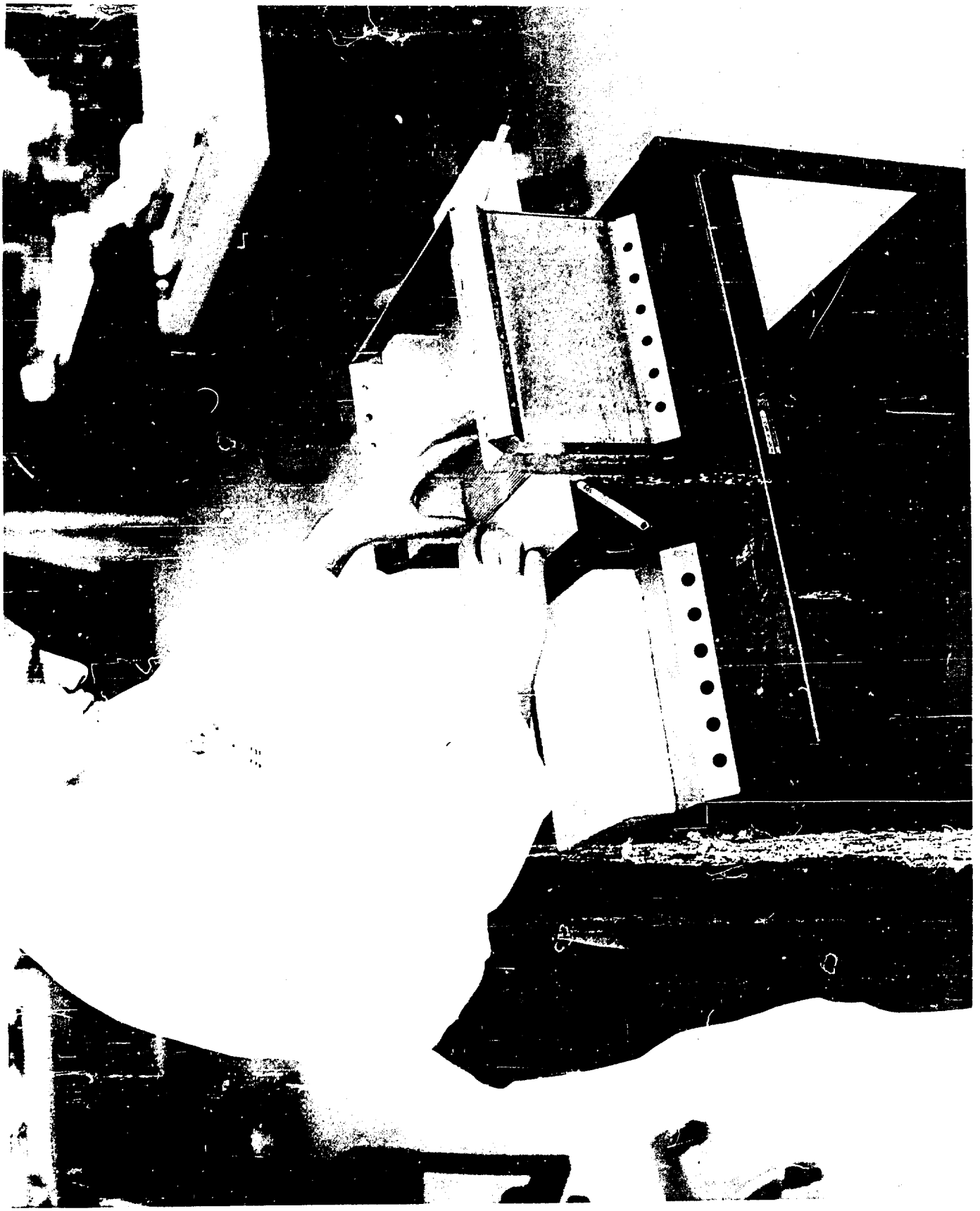

One hot-press die

Figure 9

Material Development (continued)

Figure 10 is a schematic of the modified hydraulic system. Figure 11 is a photograph of the completed panel.

3.4.2 Small Hot Press Die Experiments

Fifteen 3.0 x .3 x .3 inch bars have been hot pressed during the past quarter. All the material was flame sprayed and the majority was of composition 4. These hot pressings were run to determine optimum sintering conditions. Table IV gives sintering conditions and some physical properties for these samples.

The slope of curves in Figure 12 is taken from hot pressed samples of composition NAGS-4-Sa only. This data indicates that temperature and pressure have the greatest effect on density. Time at a constant temperature and pressure did not have an appreciable effect on the final density.

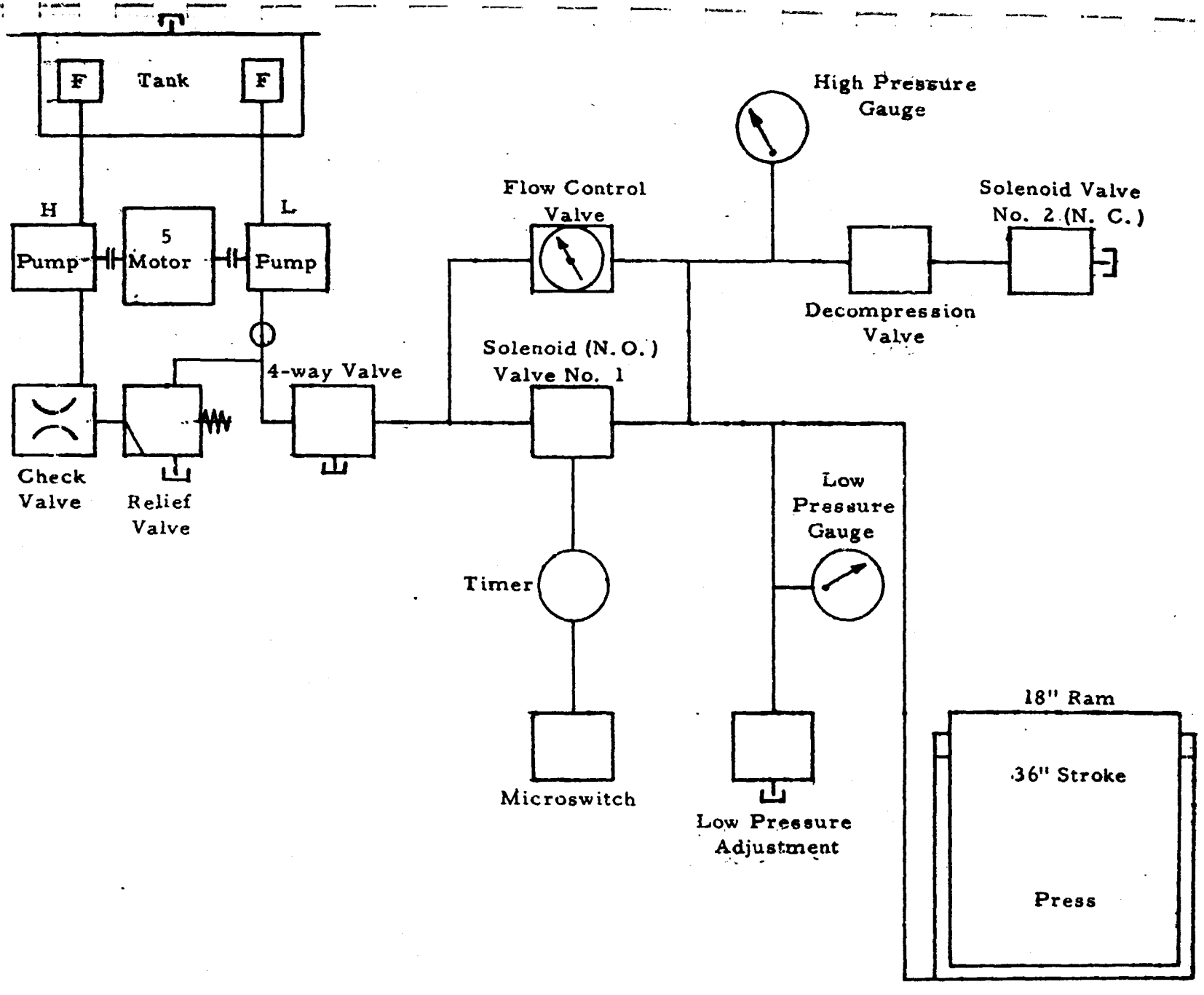

Figure 10
Hydraulic System
Airtron, a division of Litton Industries

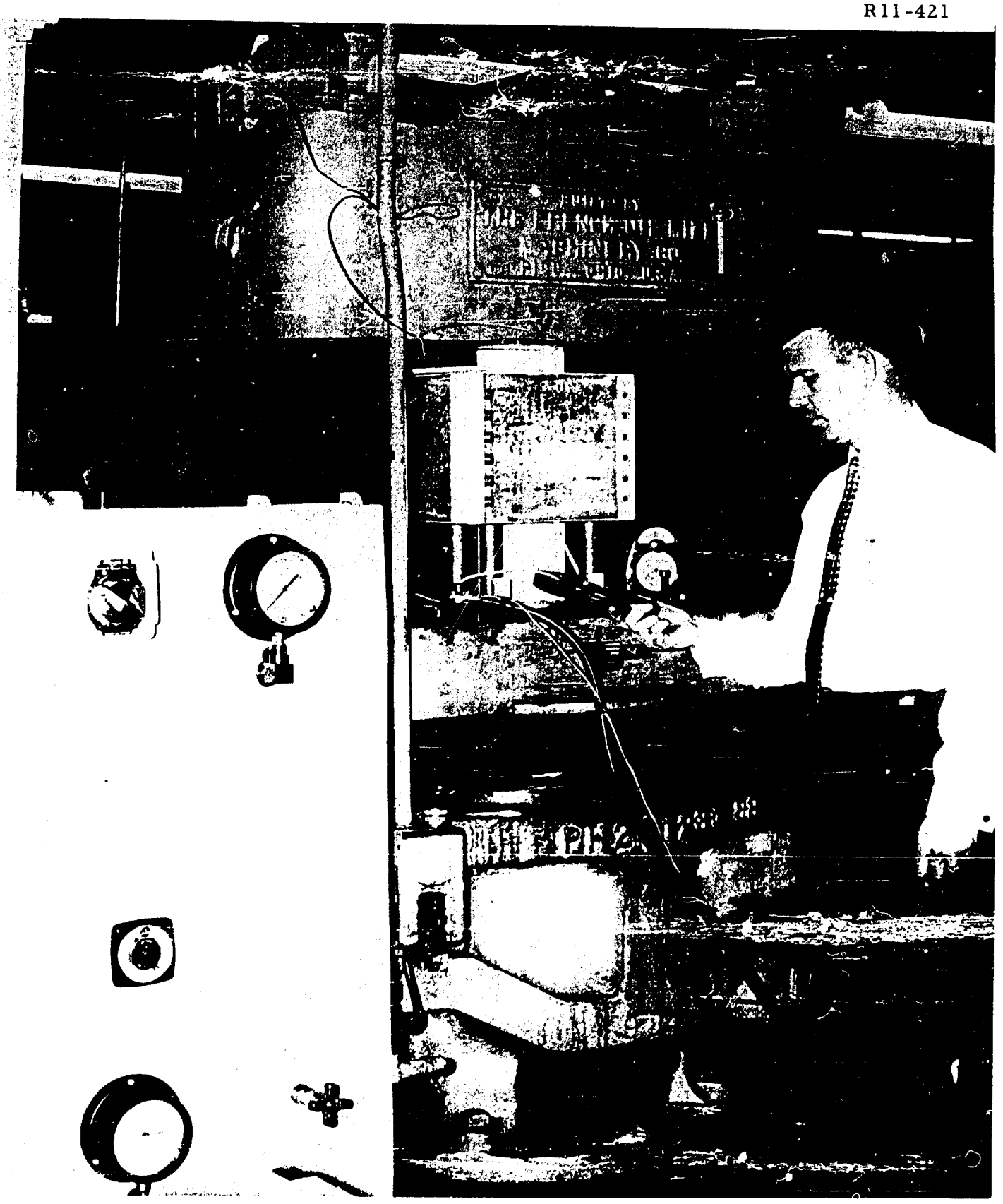

Figure 11 - Hydraulic Panel

TABLE IV

HOT PRESS CONDITIONS AND PHYSICAL DATA

Sample	Comp.	From	P	T	t	Porosity	$4\pi M_s$	T_c
HP-26	4	Sa	4000	1125	15	10.8	726	201
HP-27	4	Sa	4000	1125	30	9.46	730	203
HP-28	4	Ft	4000	1125	15	20.7	555	203
HP-29	3	Sa	4000	1125	30	10.25	---	169
HP-30	3	Ft	4000	1125	45	---	535	200
HP-31	3	Sa	4000	1125	45	9.5	---	171
HP-32	4	Sa	6000	1125	15	14.93	---	179
HP-33	3	Sa	8000	1125	30	7.16	---	169
HP-34	4	Sa	6000	1125	30	3.11	---	---
HP-35	4	Sa	8000	1125	30	3.07	---	---
HP-36	4	Sa	4000	1185	30	3.87	---	---
HP-37	4	Sa	4000	1175	30	3.07	---	---
HP-38	4	Sa	4000	1225	30	0.00	---	---
HP-39	4	Sa	4000	1200	30	0.12	---	---

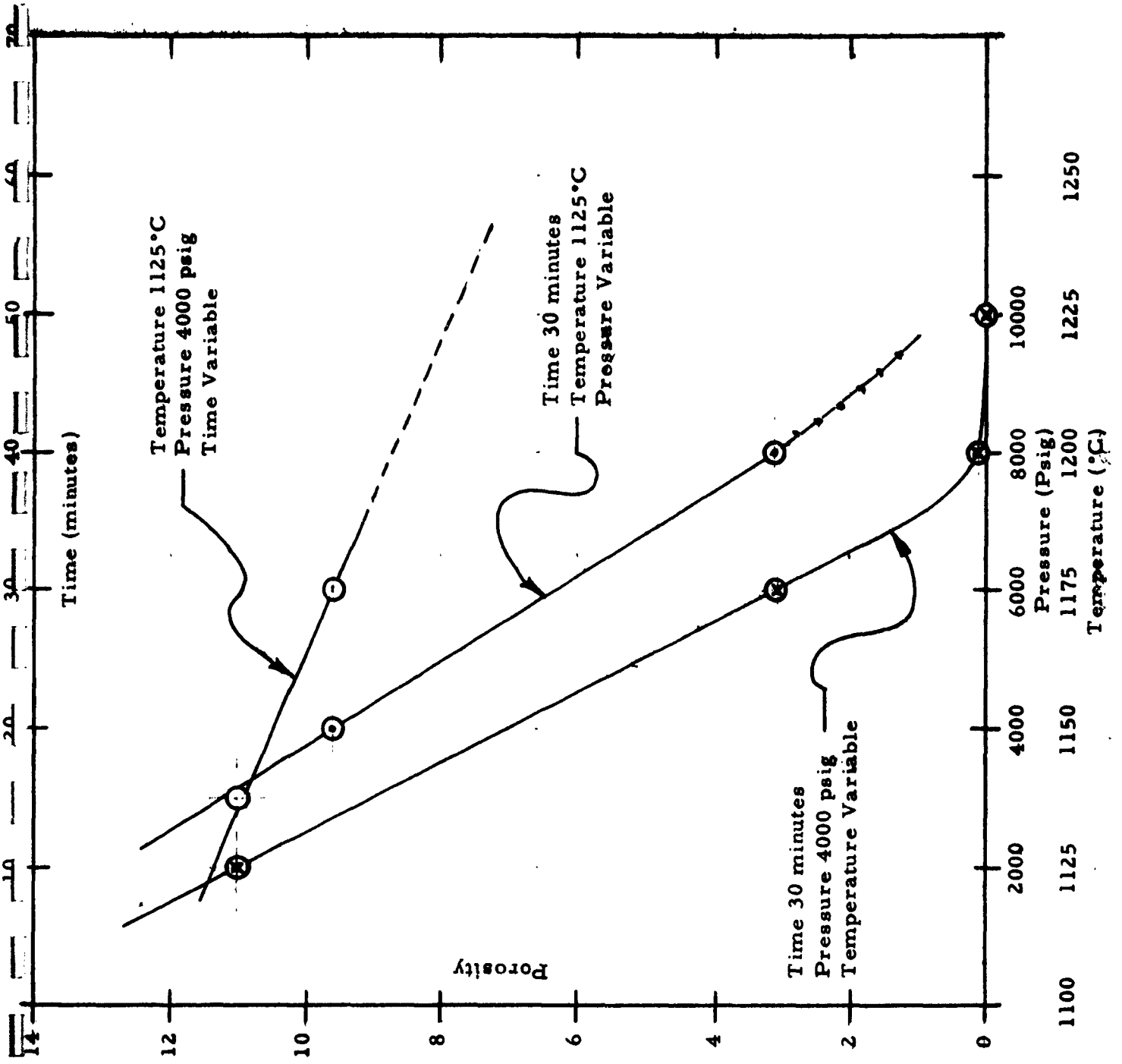

Figure 12
Hot Pressing Parameters

4. MEASUREMENT APPARATUS

4.1 Tan δ at S-band

No change has been made since the last quarter in the tan δ apparatus. We have, however, measured many samples of NAGS using various diameters. Sample diameters of 0.208, 0.104, 0.085 inches were used. The same sample was actually used where K and tan δ are given for more than one diameter in the tables. This was done by grinding the sample down after measurement at the large diameter. Tan δ data is given in Tables V and VI. The 1320°C, 1350°C, 1375°C firing temperatures for 10 hours in oxygen are designated by numbers 1128, 1115, 1149, respectively.

The discrepancy in the measured dielectric constant of 12.8 for TT-414 with reported value by the manufacturer of 11.5 has been resolved. TT-414 was remeasured with a 0.104 diameter rod and the value obtained was 11.8. This .104" sample was ground down from the .208" diameter sample which gave a dielectric constant of 12.8.

4.2 Line Shape χ' and χ'' at 3200 S-band

In the last quarter, it was reported that a TE_{111} cavity had been constructed and was awaiting evaluation. In this cavity, it was found χ'' was very sensitive to position away from the cavity wall. Spencer and Le Craw,[1] first reported this effect. Artman and Tannenwald[2] and others have also observed this effect which is due to eddy currents generated in the cavity wall. These currents give rise to a magnetic field which cannot be easily evaluated.

TABLE V

MICROWAVE PROPERTIES OF CERAMIC PROCESSED MATERIAL

	S-BAND								
	.208		.104		.085		20 Mc		X-b
Sample	K	Tan δ	K	Tan δ	K	Tan δ	K	Tan δ	g
4E1-1115	11.30	.0203	10.54	.0039	-----	-----	8.4	.0012	2.7
4E2-1115	11.18	.0195	10.45	.0042	10.33	.0031	8.68	.0050	2.6
4E3-1115	11.14	.0170	10.45	.0036	-----	-----	8.58	.0032	2.6
4E1-1128	-----	-----	9.17	.0029	-----	-----	7.1	.00104	2.6
4E2-1128	-----	-----	9.49	.0033	-----	-----	7.7	.00195	3.0
4E3-1128	-----	-----	9.74	.0031	9.59	.0020	7.35	.00097	2.6
4E1-1149	-----	too high	-----	-----	-----	-----	8.47	.0022	---
4E2-1149	-----	"	-----	-----	-----	-----	10.00	.002	---
4E3-1149	-----	"	-----	-----	-----	-----	8.3	.0006	---
4E1-1156	10.04	.0128	-----	-----	-----	-----	---	-----	---
4E2-1156	10.22	.0142	-----	-----	-----	-----	---	-----	---
4E3-1156	10.26	.0147	-----	-----	-----	-----	---	-----	---

TABLE V (Continued)

MICROWAVE PROPERTIES OF CERAMIC PROCESSED MATERIAL

	S-BAND									
	.208		.104		.085		20 Mc		X-band	
Sample	K'	Tan δ	K'	Tan δ	K'	Tan δ	K	Tan δ	g	ΔH
4P1-1115	11.02	.0140	10.14	.0031	-----	-----	8.6	.0008	2.7	410
4P2-1115	11.26	.0156	10.62	.0039	10.46	.0022	8.85	.0006	2.5	420
4P3-1115	11.40	.0132	10.64	.0027	-----	-----	8.75	.0008	2.6	420
4P1-1128	-----	-----	9.12	.0019	-----	-----	7.6	.00095	2.6	440
4P2-1128	-----	-----	10.02	.0029	9.98	.0019	8.27	.00089	2.6	465
4P3-1128	-----	-----	-----	-----	-----	-----	8.10	.0019	2.6	465
4P1-1149	-----	too high	-----	-----	-----	-----	10.6	.002	---	---
4P2-1149	-----	"	-----	-----	-----	-----	10.4	.0036	---	---
4P3-1149	-----	"	-----	-----	-----	-----	8.93	.0081	---	---
4P1-1156	10.26	.0106	-----	-----	-----	-----	---	-----	---	---
4P2-1156	10.98	.0137	-----	-----	-----	-----	---	-----	---	---
4P3-1156	11.05	.0102	-----	-----	-----	-----	---	-----	---	---

TABLE V (Continued)

MICROWAVE PROPERTIES OF CERAMIC PROCESSED MATERIAL

	S-BAND											
	.208		.104		.085		20 Mc		X-band		S-band	
Sample	K	Tan δ	K	Tan δ	K	Tan δ	K	Tan	g	ΔH	g	ΔH
4G1-1115	11.50	.0120	10.75	.0025	-----	-----	9.0	.0016	2.4	325	2.6	135
4G2-1115	10.82	.0099	10.64	.0020	10.47	.0014	8.45	.0016	2.9	280	3.2	260
4G3-1115	11.38	.0075	10.22	.0025	-----	-----	8.97	.0040	2.5	295	2.7	167
4G1-1128	-----	-----	-----	-----	-----	-----	8.5	.00133	2.7	375	2.8	320
4G2-1128	-----	-----	-----	-----	-----	-----	8.3	.00086	2.6	530	2.9	335
4G3-1128	-----	-----	10.25	.0016	10.08	.0011	8.18	.0012	3.0	430	---	---
4G1-1149	11.14	.017	-----	-----	-----	-----	10.38	.0046	---	---	2.7	200
4G2-1149	11.14	.0035	-----	-----	-----	-----	9.35	.0015	---	---	3.0	220
4G3-1149	11.52	.0091	-----	-----	-----	-----	10.31	.0040	---	---	2.9	310
4G1-1156	11.12	.0094	-----	-----	-----	-----	----	-----	---	---	---	---
4G2-1156	10.82	.0105	-----	-----	-----	-----	----	-----	---	---	---	---
4G3-1156	10.74	.0082	-----	-----	-----	-----	----	-----	---	---	---	---

TABLE V (Continued)

MICROWAVE PROPERTIES OF CERAMIC PROCESSED MATERIAL

	S-BAND									
	.208		.104		.085		20 Mc		X-band	
Sample	K	Tan δ	K	Tan δ	K	Tan δ	K	Tan δ	g	ΔH
4H1-1115	11.50	.0171	10.80	.0068	-----	-----	9.15	.026	2.7	360
4H2-1115	11.45	.0191	10.78	.0087	10.62	.0084	9.45	.043	2.7	365
4H3-1115	11.50	.0191	10.69	.0065	-----	-----	9.30	.037	2.7	375
4H1-1128	-----	-----	10.67	.0054	-----	-----	8.5	.0104	2.9	350
4H2-1128	-----	-----	10.08	.0072	-----	-----	8.73	.0183	2.9	370
4H3-1128	-----	-----	10.64	.0063	10.49	.0056	9.27	.0264	2.8	385
4H1-1149	-----	too high	-----	-----	-----	-----	8.95	.035	---	---
4H2-1149	-----	"	-----	-----	-----	-----	9.77	.042	---	---
4H3-1149	-----	"	-----	-----	-----	-----	11.9	.072	---	---
4H1-1156	11.59	.0174	-----	-----	-----	-----	---	-----	---	---
4H2-1146	11.54	7.018	-----	-----	-----	-----	---	-----	---	---
4H3-1146	11.26	7.018	-----	-----	-----	-----	---	-----	---	---

TABLE VI

MICROWAVE PROPERTIES OF HOT PRESSED MATERIALS

	S-BAND									
	.208		.104		.085		20 Mc		S-band	
Sample	K	Tan δ	K	Tan δ	K	Tan δ	K	Tan δ	g	ΔH
HP-26	9.92	.0114	9.20	.0092	---	---	7.20	.0054	---	---
HP-27	10.27	.0108	9.51	.0082	---	---	14.7	.0064	---	---
HP-28	8.65	.0085	8.21	.0049	---	---	5.8	.0328	2.9	300
HP-30	----	----	7.18	.0042	---	---	---	-----	---	---
HP-32	----	can't see	----	-----	---	---	---	-----	---	---
HP-33	----	"	----	-----	---	---	7.55	.0107	---	---
HP-34	----	----	----	-----	---	---	6.93	.0047	---	---
HP-35	----	----	----	-----	---	---	8.07	.0049	---	---
HP-36	----	----	----	-----	---	---	6.78	.0070	---	---
HP-37	----	----	----	-----	---	---	6.63	.0049	---	---
HP-38	----	----	----	-----	---	---	---	-----	---	---
HP-39	----	----	----	-----	---	---	8.4	.0066	---	---

Measurement Apparatus (continued)

In order to avoid wall effects and possible errors, a TE_{102} cavity was constructed. A ferrite sphere placed at the center of this cavity, see Figure 13, is at a point of maximum h_{rf} and zero electric field. Because the ferrite is far from any wall, the above mentioned effects do not occur.

For a TE_{102} cavity, χ'' and χ' are given by:[2]

$$\chi'' = \left(\frac{1}{Q_L{}^s} - \frac{1}{Q_L{}^e}\right) \frac{\frac{V}{\Delta V}}{4\left[1 - \left(\frac{\lambda_o}{2a}\right)^2\right]}$$

$$\chi' = \frac{-\Delta F}{F_o} \frac{V}{\Delta V} \frac{1}{2\left[1 - \left(\frac{\lambda_o}{2a}\right)^2\right]}$$

Where $Q_L{}^s$ and $Q_L{}^e$ are the loaded Q of the cavity with and without samples respectively. F_o is the cavity resonant frequency; ΔF is the change in cavity resonant frequency upon sample insertion; V and ΔV are the respective cavities and sample volumes, λ_o is the resonant frequency free space wavelength and "a" is the cavity width.

If the cavity is placed between the poles of an electromagnetic, χ'' and χ' can be measured as a function of magnetic field. To measure ΔF and $\frac{1}{Q_L{}^s} - \frac{1}{Q_L{}^e}$, the cavity must be placed in the bridge used to measure K and tan δ.

χ'' was measured for several samples. Figures 18, 19, 20, and 21 are curves of χ'' vs. magnetic field. TT-414 was measured and is shown in Figure 18.

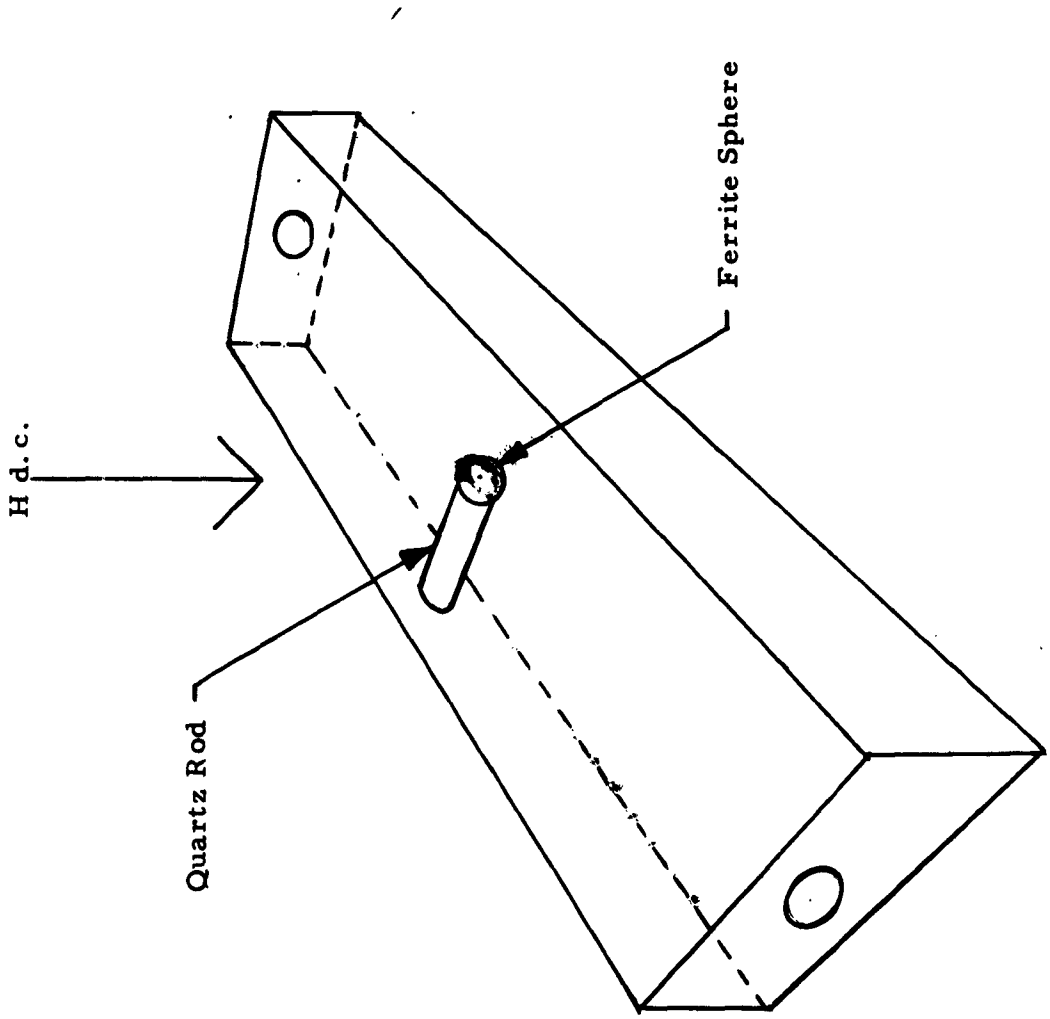

Figure 13
TE_{102} Cavity

Measurement Apparatus (continued)

Because χ' is so small and difficult to even observe, except near resonance, it was not measured.

4.3 High Power Loss vs. Peak Power

The high power setup is now complete. During the final period, measurements will be made of loss vs. peak power of an S-band phase shifter containing a large sample (1" x 1" x 6") of NAGS.

4.4 Phase Shift Measurements

During this last report, we attempted to measure phase shift using small samples at S-band in a doubly ridged waveguide. Even with a micrometer capable of measuring .0001 of an inch, we were unable to measure any phase shift.

We then attempted to measure phase shift in a small X-band waveguide (i.d. .400 inches x .900 inches).

A .900 inch long sample with a diameter of .300 inches was used. Aluminum oxide tapers were used for matching. A coil was wrapped around the guide so that a longitudinal field could be applied. Data were obtained for several NAGS samples as well as for TT-414. The data are given in Table VII.

During the final period, measurements will be made using large samples of NAGS (1" x 1" x 6 inches) in an S-band rectangular waveguide (Reggia-Spencer) phase shifter.

TABLE VII

PHASE SHIFT AND INSERTION LOSS DATA

Material	Diameter of Rod	Phase Shift	Loss
TT-414	.300	60°	.3 db
TT-414	.285	57°	.25 db
TT-414	.270	14°	.05 db
NAGS-4E1-1128	.300	10°	.55 db
NAGS-E1-1149	.300	27°	.75 db
NAGS-4E2-1128	.300	12°	.55 db
NAGS-4E3-1128	.300	13°	.57 db
NAGS-4P1-1128	.300	12°	.34 db
NAGS-4P2-1128	.300	20°	.52 db
NAGS-4P3-1128	.300	19°	.48 db
NAGS-4P1-1149	.300	21°	.55 db
NAGS-4P2-1149	.300	33°	.95 db
NAGS-4P3-1149	.300	31°	.75 db
NAGS-4G1-1128	.300	29°	.28 db
NAGS-4G2-1128	.300	22°	.28 db
NAGS-4G2-1149	.300	27°	.45 db
NAGS-4G3-1128	.300	24°	.2 db
NAGS-4H1-1128	.300	30°	.3 db
NAGS-4H2-1128	.300	33°	.42 db
NAGS-4H3-1128	.300	31°	.4 db

All samples were 0.900 inches long.

Measurement Apparatus (continued)

Figure 14 contains a plot of phase shift and insertion loss versus current for TT-414. The sample was 6 inches long by .925 inches square. Aluminum oxide tapers were used to match into the ferrite. The ferrite and oxide were placed in WR-229 which has inside dimensions 2.290 inches by 1.145 inches. The curve of phase shift versus current follows the usual pattern, except that it decreases rather than levels off as the current increases. This can be attributed to moding because of too large a ferrite sample. The loss versus current curve bears this out; one can see that the phase shift is dropping where the loss has begun to rise rapidly. During the next quarter, a smaller sample will be measured.

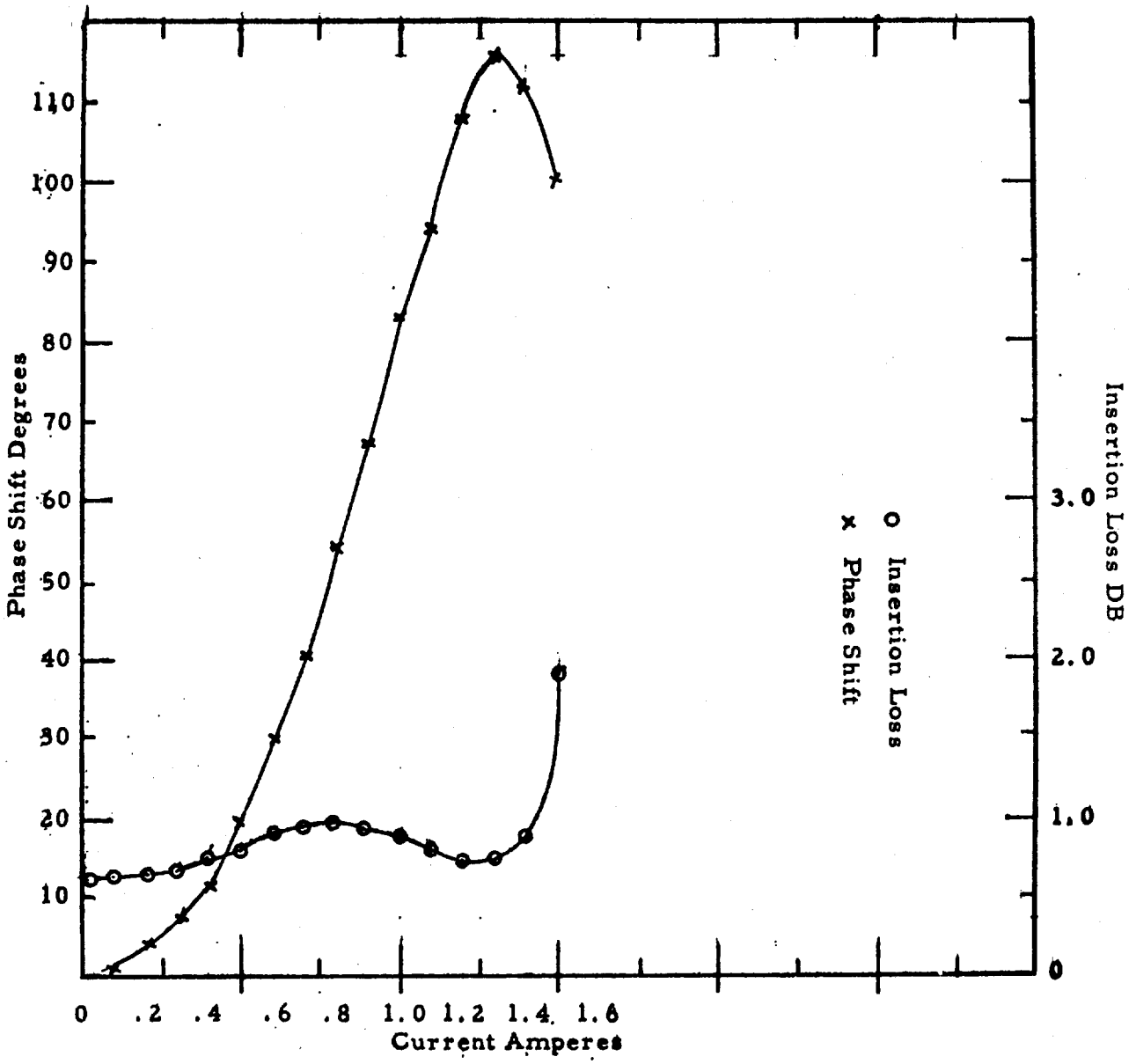

Figure 14
Phase Shift and Loss vs. Current for TT-414

5. DISCUSSION OF RESULTS

5.1 Introduction

The original contract specifications were formulated with the aim of producing a material suitable for use in a Reggia-Spencer phase shifter which will operate at high power levels. The new material is to have properties similar to those of TT-414, with a Curie point of 200°C. The higher Curie point is desired so the device can handle high power. At the present time, all of the low power measurements have been completed and the specific contract requirements have been met. However, the problem of low field magnetic loss has limited the phase shifter work. Ceramic processing, flame spraying, and hot pressing work was carried out during the past quarter to gain an insight to the low field loss problem. An operable material should have low field χ'' comparable to TT-414.

5.2 Detailed Discussion

5.2.1 Curie Point and Saturation Magnetization

As described in the previous Interim Reports, several compositions in the nickel gallium aluminum ferrite system were prepared containing various substitutions and aluminum to gallium ratios, e.g., NAGS-4.

$$(NiO)_{0.98}(MnO_2)_{0.02}(Ga_2O_3)_{0.124}(Al_2O_3)_{0.364}(Fe_2O_3)_{0.463}$$

Substitution 0.975 moles, Al/Ga = 2.95

Composition 4 has a Curie point in the vicinity of 200°C, see Table I, and a $4\pi M_s$ variable over a range similar to TT-414. The

Discussion of Results (continued)

$4\pi M_s$ values for TT-414 measured at Airtron have varied from 650 g to 830 g, whereas NAGS-4 varies from 550 g to 810 g.

The Curie point variations observed in materials of the same initial composition is attributed to the iron picked up during milling. The ceramic processing of Compositions 4E1 - 4H3 yielded Curie points ranging from 187°C to 210°C, see Table I, which are directly proportional to Fe^{+++}, see Table VIII, content. Figure 15 shows that stoichiometric composition NAGS-4 will have a Curie point of 195°C minimum.

The large variations in $4\pi M_s$ are still not completely understood but can be empirically related to porosity and linewidth data as shown in Tables I and V. The saturation per gram is highest in low porosity, narrow linewidth materials.

The Curie point and $4\pi M_s$ properties for NAGS-4 are adequate, but a suitable device material must combine these properties with low loss.

5.2.2 S-band Tanδ and Related Magnetic Loss

5.2.2.1 Ceramic Processed Material

S-band tan δ results obtained for 0.208 diameter samples are not true measurements of dielectric loss. These samples are large enough to see magnetic fields in the TM_{012} cavity. Reducing the sample diameter until the tan δ values are constant with

TABLE VIII

IRON ANALYSIS DATA

Sample	$\%Fe_2O_3$ Expected	$\%Fe_2O_3$ Analyzed	Fe_2O_3 Grams Pick-up	Moles Fe^{+++}	Total Trivalent	Deviation from Stoichiometry In Grams
4E1	35.31	37.02	8.3	.999	1.975	-2.86
4E2	35.31	36.77	7.0	.987	1.963	-4.23
4E3	35.31	37.47	10.4	1.018	1.994	-0.68
4P1	35.31	37.48	10.4	1.018	1.994	-0.68
4P2	35.31	37.08	8.4	1.000	1.976	-2.85
4P3	35.31	37.15	8.75	1.003	1.979	-2.40
4G1	35.31	38.32	14.62	1.054	2.030	+3.50
4G2	35.31	38.31	14.62	1.054	2.030	+3.50
4G3	35.31	38.31	14.62	1.054	2.030	+3.50
4H1	35.31	38.52	15.65	1.063	2.039	+4.55
4H2	35.31	39.30	19.70	1.098	2.075	+8.60
4H3	35.31	39.35	19.80	1.099	2.076	+8.70

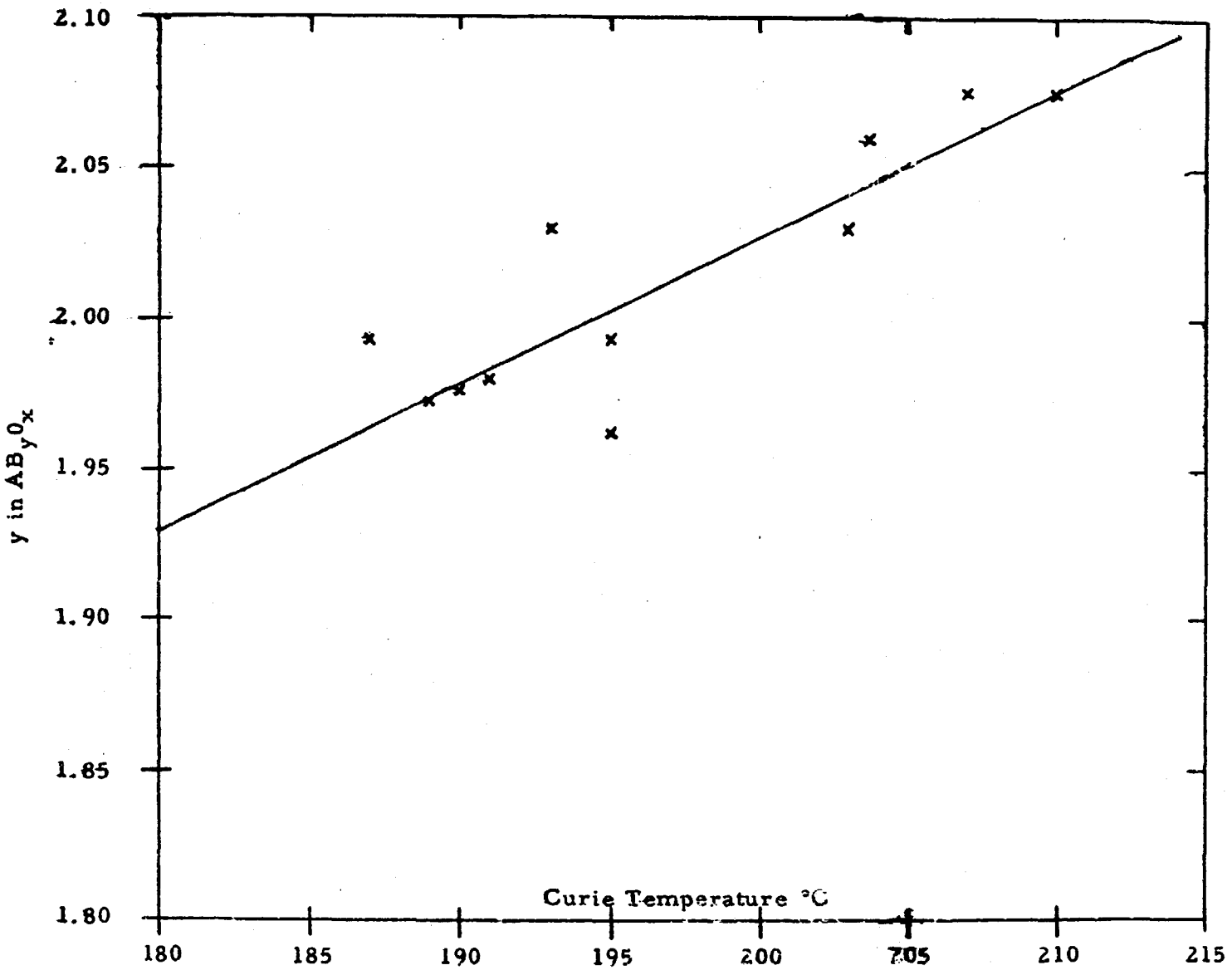

Figure 15
Curie Point vs. Composition

R11-421

Discussion of Results (continued)

diameter gave a more valid indication of true dielectric loss. The difference between the true dielectric loss and the "apparent loss" measured on .208 samples can be qualitatively compared to magnetic loss. Figure 16 shows the variation of tan δ with diameter for several samples fired at 1350°C for 10 hours.

Dielectric loss tangents less than 0.003 have been measured on the 12 hour milled (4E) and 24 hour milled (4P) series, and less than 0.002 on the 48 hour milled (4G) series. The 96 hour milled (4H) series has an average S-band tan δ of about 0.007. Figure 17 and Table VIII show the change in dielectric loss with iron content.

The dielectric loss values are taken from .085 diameter samples. As expected, Figure 17 shows that the iron excess 96 hour milled (4H) series has the highest S-band tan δ. Figure 17 also indicates that samples near stoichiometry should have dielectric losses less than 0.001. These values for S-band tan δ are well under the contract requirement of 0.005, however, extremely high magnetic losses on the majority of the conventionally processed materials eliminates the use of the material in a phase shifter. As previously stated, the magnetic loss can be qualitatively looked at as the difference between the .208 and .104 or .085 S-band tan δ's. The 48 hour milled (4G) series, for all firings, had the lowest .085 tan δ's and, also, the smallest relative magnetic loss, see Table V. A series of absorption curves (χ'' vs. H d.c.) were run on

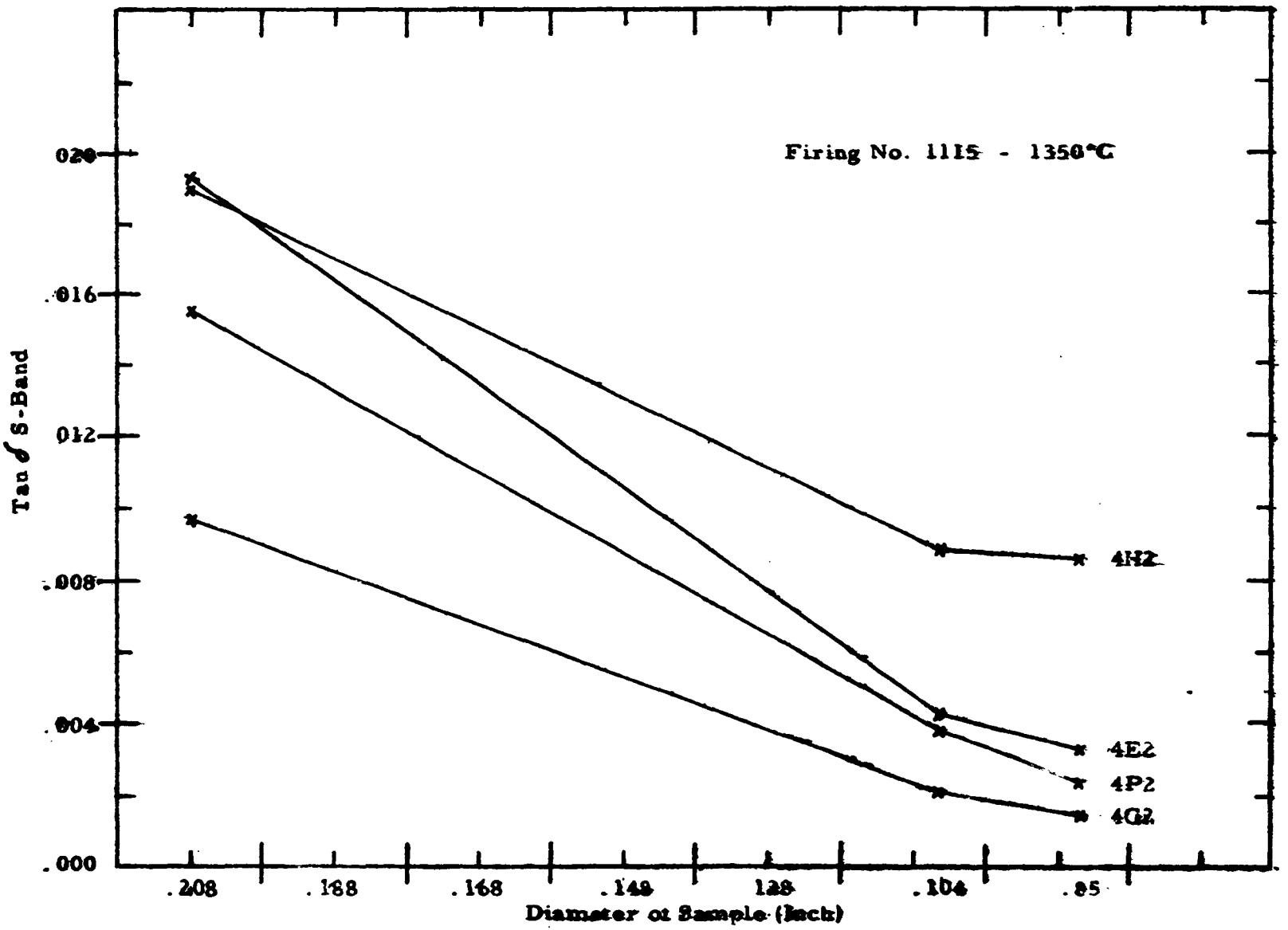

Figure 16 - S-Band Tan δ vs. Sample Diameter

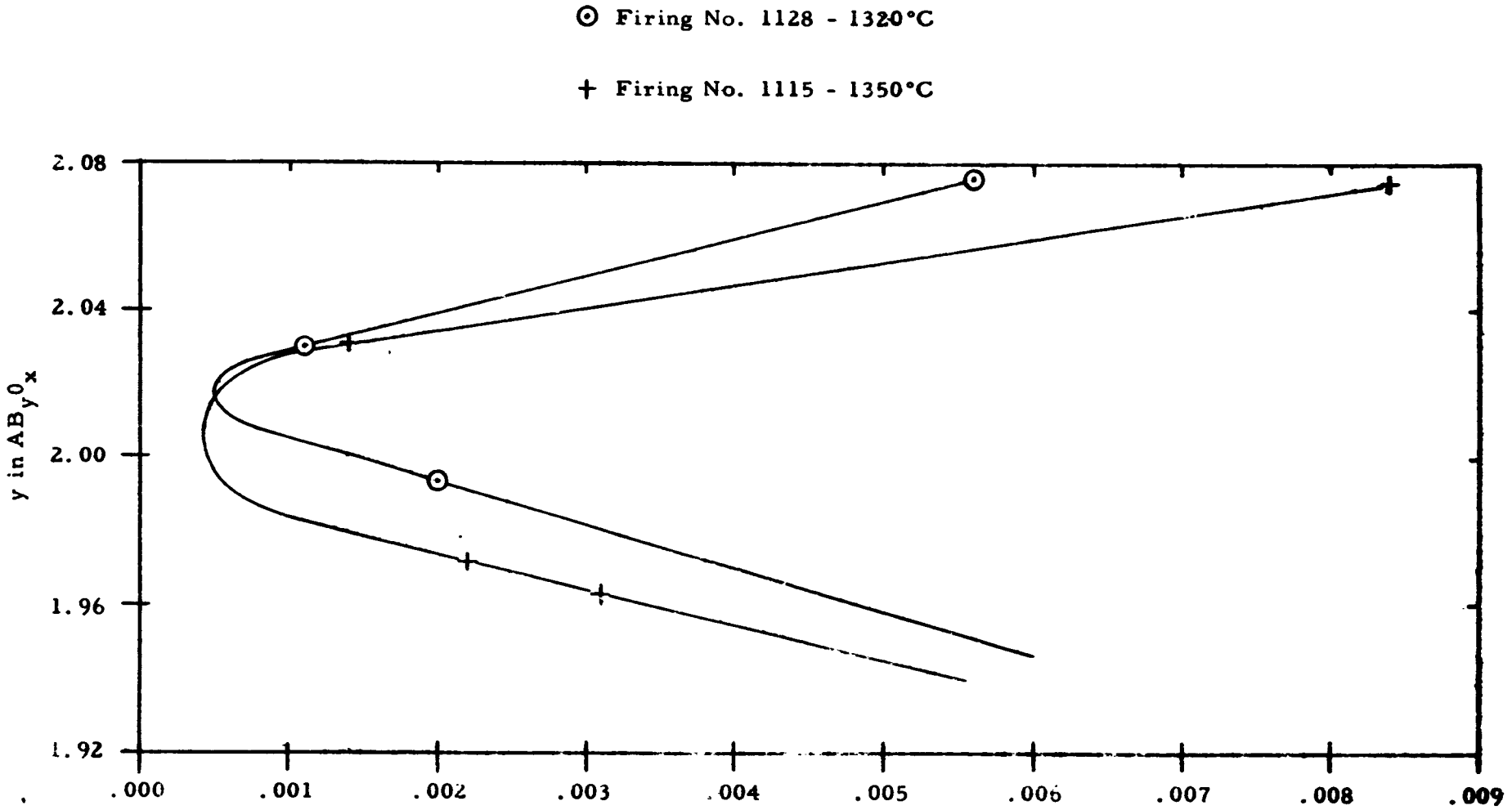

Figure 17

S-Band Tan δ vs. Composition

Discussion of the Results (continued)

samples from the 48 hour milled (4G) series, Figures 18, 19, 20, and 21. These curves were taken to:

1. Compare χ'' to S-band tan δ for NAGS and TT-414 samples.

2. Observe any loss valley in a region of H where a phase shifter would operate.

3. Observe if there was any low field loss due to linewidth.

4. Measure S-band ΔH.

The χ'' for TT-414 is less than .025 from H = 0 to H = 650 gauss, see Figure 15. The best NAGS materials at H = 0 has a χ'' greater than 10 times that of TT-414 and the average zero field χ'' is 20 times that of TT-414. The average ratio of S-band tan δ of the 48 hour milled (4G) series (taken from .208 diameter samples which includes all the loss) is also 20 times the S-band tan δ of TT-414 (0.010 average for 4G series compared to 0.005 for TT-414). Only one sample, 4G1-1115, had a loss comparable to that of TT-414 below resonance. The low loss region for 4G1-1115 occurred between H = 325 to H = 375 gauss. This particular sample had the highest $4\pi M_s$, lowest "g" and ΔH of all the ceramic processed samples of the composition 4 series. It suggests the possible use of higher $4\pi M_s$ material fired to lower densities to reduce low field loss, and still retain the necessary phase shift.

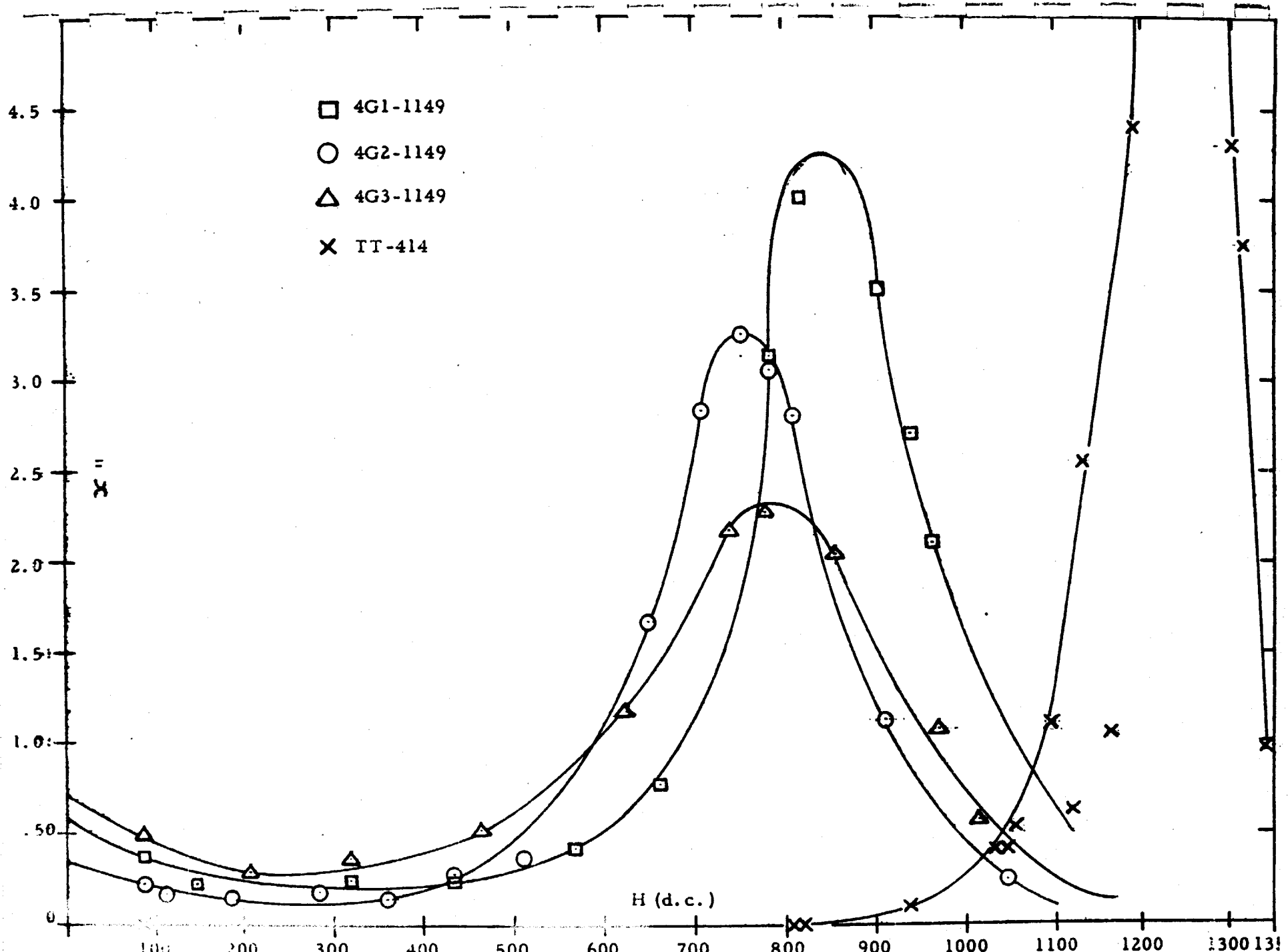

Figure 18 - χ'' vs. H (d.c.)

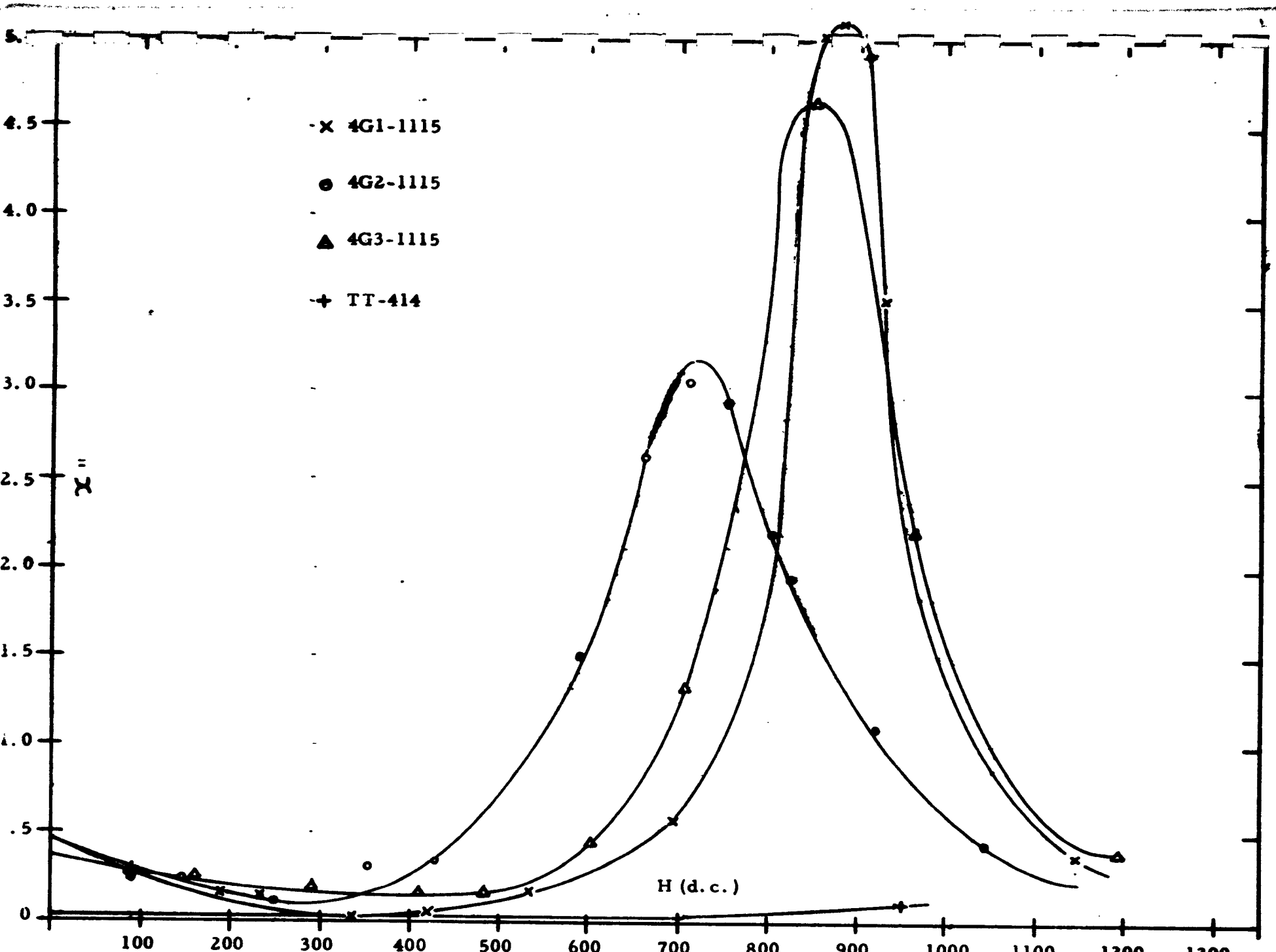

Figure 19 - χ'' vs. H (d.c.)

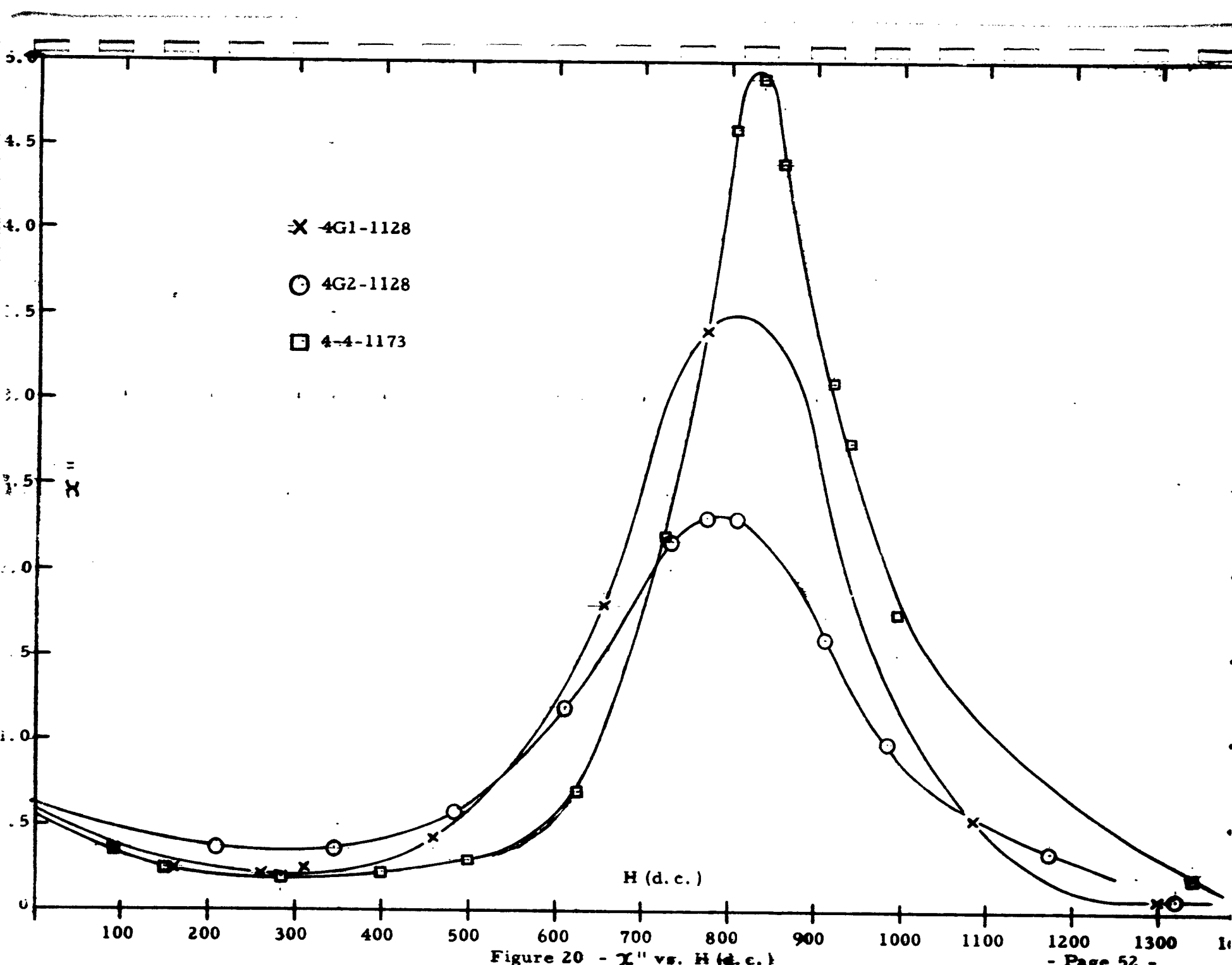

Figure 20 - χ" vs. H (d.c.)

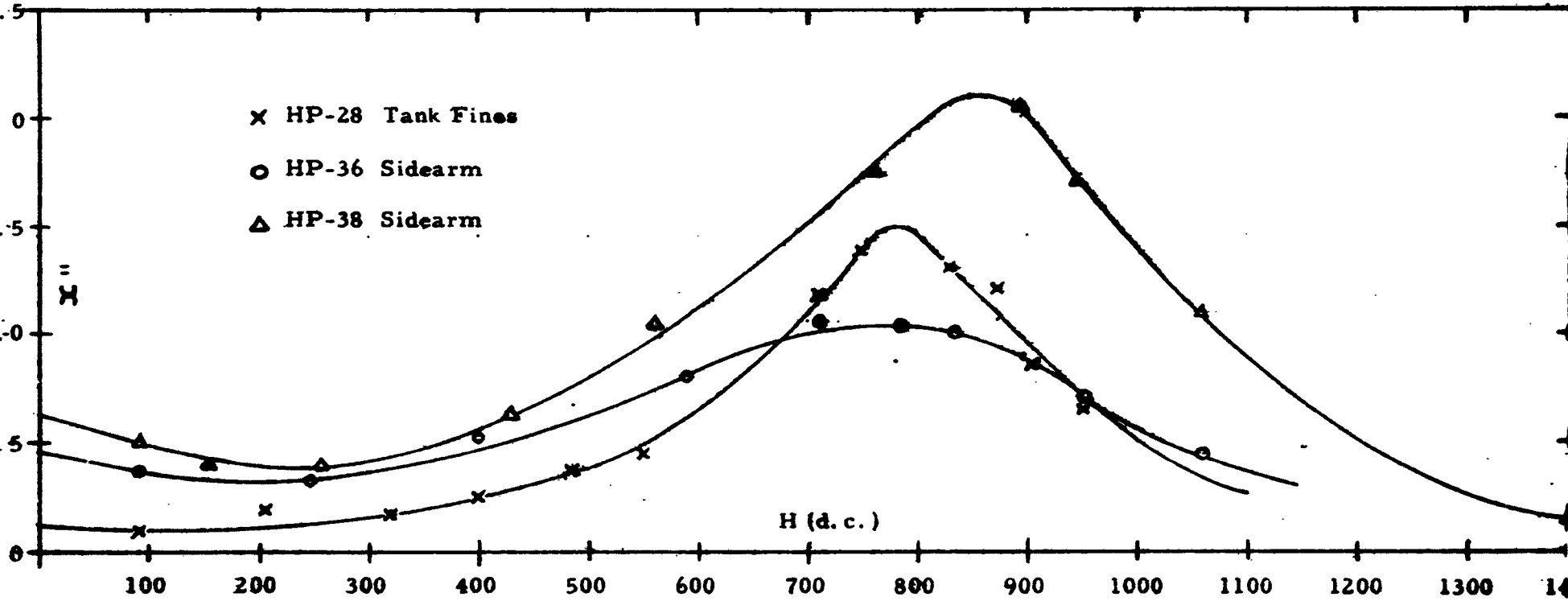

Figure 21 - χ'' vs. H (d.c.)

Discussion of Results (continued)

Figure 22, a plot of .208 tan δ vs. B in AB_yO_x, also indicates that the magnetic loss may be reduced by approaching a stoichiometric composition.

The 96 hour milled (H) series cannot be realistically compared to the 12 hour milled (E), 24 hour milled (P), and 48 hour milled (G) series because of the large excess iron over stoichiometry shown by analysis, see Table VII, and dielectric loss (.085 diameter samples, Figure 17 and Table V). During the next quarter, a 96 hour milled, iron compensated, composition 4 batch will be processed.

5.2.3 Flame Spray - Hot Pressed Materials

The flame sprayed sidearm hot pressed material had S-band tan δ on the .104 inch samples ranging from .0082 to .0092. These values were higher than the specifications required. These materials were NiO rich which might have accounted for some of the loss. The results are not as good as those obtained with conventional processing. In fact, they were not as good as one usually observes for flame sprayed material.

The absorption curves of hot pressings, numbers 36 and 38, show low resonance peaks and rather broad linewidths with only slight valleys occurring in the 150 to 300 gauss range. The zero field loss of these materials averaged .58 χ'' units. As mentioned in the section on flame spraying, batch 7-1 will be an attempt to bring the batch further

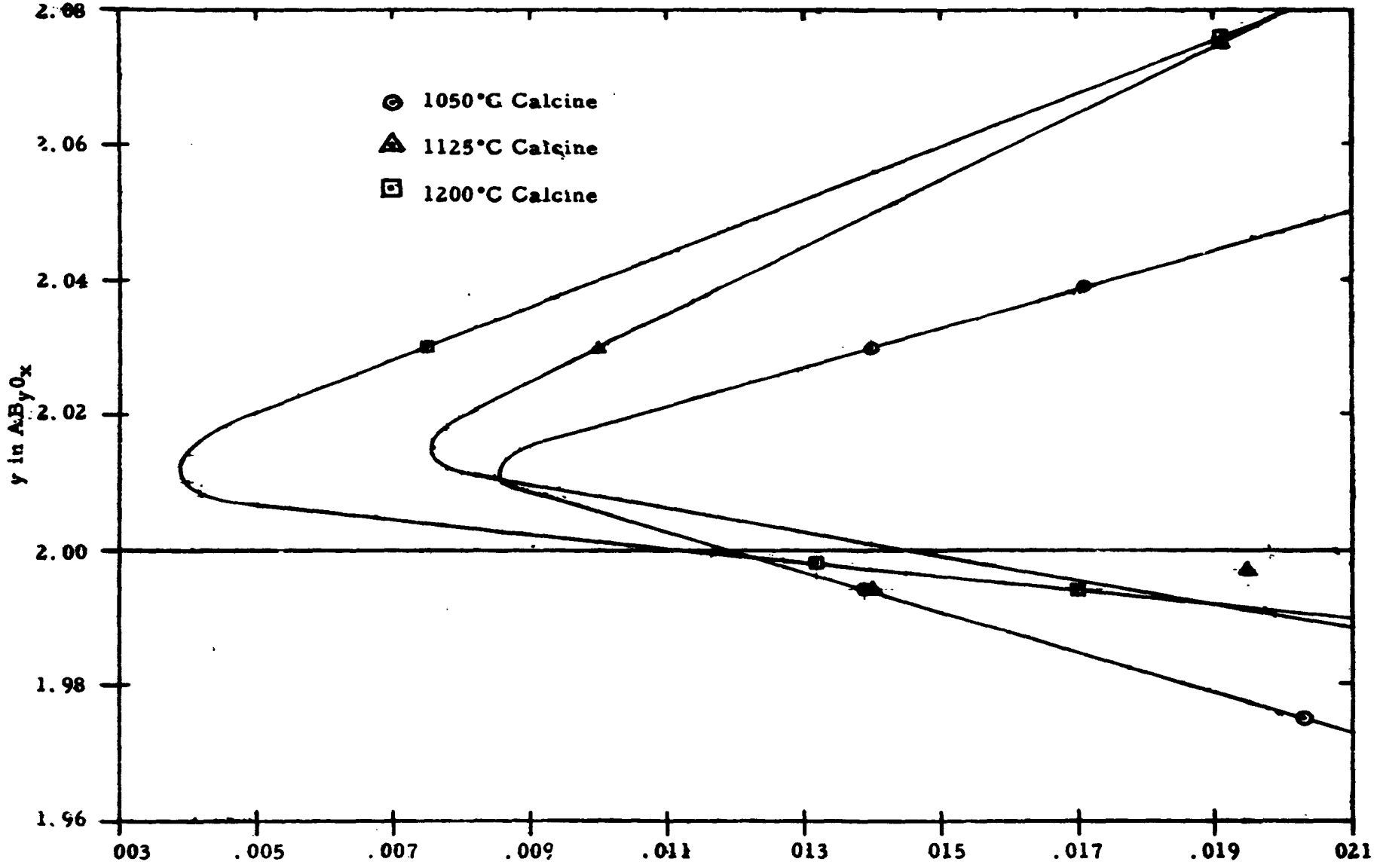

Figure 22
S-Band Tan δ vs. Composition

Discussion of Results (continued)

toward stoichiometry. Tests are presently being made on this material.

As described above, the flame sprayed, hot pressed material taken from the sidearm did not have reduced S-band tan δ as other conventionally prepared material. However, HP-28, prepared from material collected in the water, that is, the ultra fines, had a .208 S-band tan δ of 0.0086 and a zero field χ'' of 0.125. Also, the χ'' remained at 0.125 until H = 250 gauss. HP-28 had 20 percent porosity and resulting S-band ΔH of 300. A dense, hot pressed fine particle material could have a large region of low loss and suitable phase shift. It is also possible to flame spray and hot press a 20 percent porosity material having a higher $4\pi M_s$ to give the required phase shift. This is done by simply adjusting the Al to Ga ratio so the Curie point remains constant.

5.2.4 Phase Shift

Study of the phase shift and loss data on Table VII indicates the possible advantage of long milling time. This loss measurement is almost exclusively a measure of the magnetic loss. Due to the placement in the waveguide, the dielectric contribution to the recorded loss is very small. It is noted that the best losses recorded are for the 48 and 96 hour milled materials. It can be seen that the extended milling, even though it is iron excess, had not adversely affected the phase shift and loss of the material.

A plot of the peak of the absorption curve vs. saturation

Discussion of Results (continued)

magnetization, Figure 23, shows higher absorption peaks with higher saturations. This plot is data for all calcining temperatures and all firings. There are only a few points presently available to compare phase shift with the peak of the absorption curve. The available data are plotted in Figure 24. The phase shift increases with an increase in the peak of the absorption curve. Examination of the absorption curves shows that the high saturation (700-800 gauss) materials did not effect the low field loss. It is apparent that additional phase shift data on the high saturation materials should be made. If the phase shift data obtained follows the trends indicated, it would be desirable to make a material with a saturation magnetization between 800 and 1000 gauss.

Figure 25, which is a plot of ferromagnetic linewidth at S-band vs. absorption peak, indicates the narrow linewidth gives more workable area below resonance for construction of a low field device.

Absorption curves on a few hot pressed samples were also run. The one available point of saturation magnetization vs. absorption peak is also plotted on Figure 23. The point fits the curve obtained for the conventionally sintered materials. This also indicates that it may be necessary to flame spray a material that will yield a high saturation (approximately 800 gauss) in order to increase the absorption peak and the phase shift and decrease the linewidth.

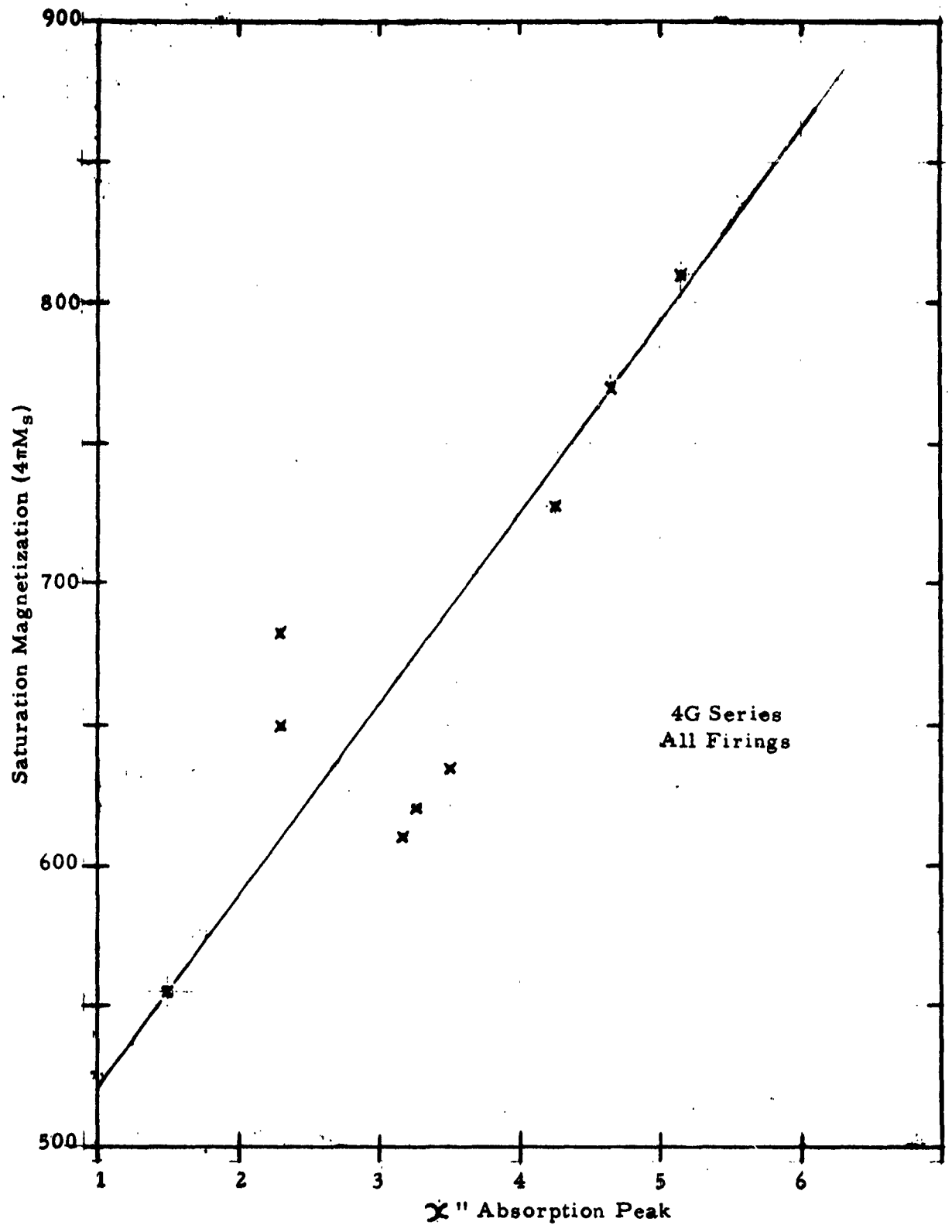

Figure 23
Saturation Magnetization vs. Absorption Peak

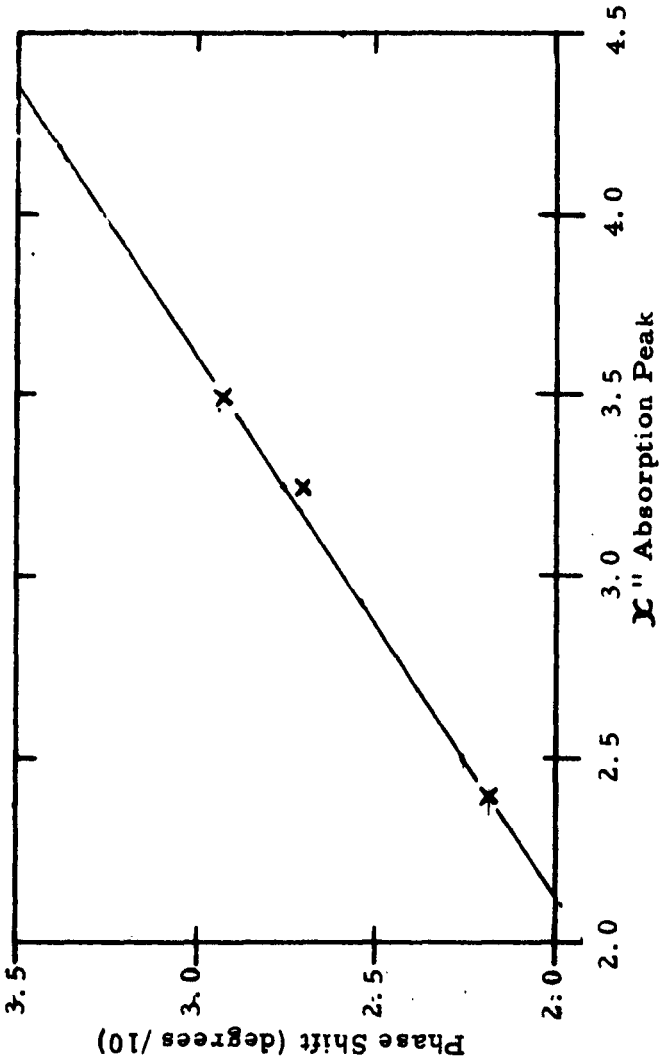

Figure 24
Phase Shift vs. Absorption Peak

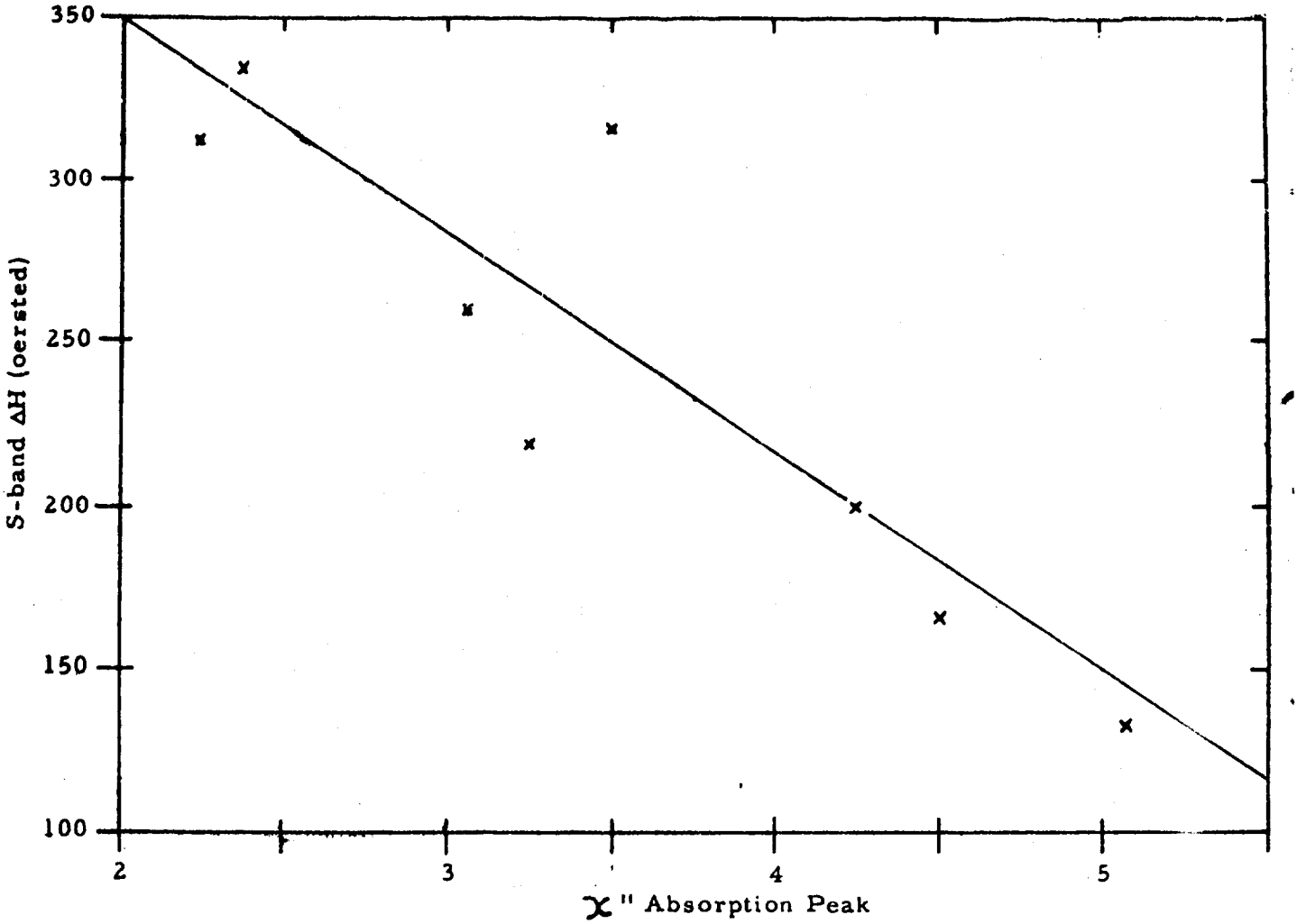

Figure 25
S-Band ΔH vs. Absorption Peak

6. SUMMARY

The material to be developed under this contract is to have the following characteristics:

a. Curie temperature 200°C minimum.

b. Minimum density 95 percent of theoretical.

c. Dissipation factor 0.005.

d. Suitability for a below resonance S-band phase shifter operating at peak powers of 250 kilowatts.

Some materials developed during this study in the nickel gallium aluminum ferrite system fulfill requirements (a), (b), and (c). It is the phase shifter requirement which requires further work.

If we try to use the material in a phase shifter operating near zero field, we find low field loss is excessive in samples prepared so far. This is the type of application where one would directly replace a material like TT-414. The data obtained suggest, however, that low field loss can be reduced by using flame sprayed, hot pressed material with a porosity near 20 percent; for example, sample HP-28. Also, material which is close to stoichiometry should have reduced low field loss.

Further work will be directed toward preparation of hot pressed samples using very fine particles; the processing will be controlled to yield low density material. The loss in effective magnetization through high porosity will be compensated for by increasing $4\pi M_s$ of the material. This will have the additional benefits of decreasing the linewidth and decreasing the "g" factor; both

Summary (continued)

changes will increase phase shift.

There is an alternative solution to the phase shifter problem. Some of the materials with excessive low field loss have a deep valley between the low field loss peak and the resonance peak (sample no. 4G1-1115, for example). The phase shifter can be designed with a permanent bias so that it operates in the region of the valley between the two loss peaks.

Both of the above approaches are now being tried.

The behavior of the samples under high power must await a solution to the low field problem or the satisfactory design of a phase shifter incorporating a biasing field. This will be the major goal of the work performed in the remaining time of the contract.

7. PROGRAM FOR THE NEXT INTERVAL

The work during the next interval will be primarily directed toward reducing or possibly eliminating low field loss and still retain a 200°C Curie point and satisfactory phase shift characteristics. Materials, which have been processed conventionally and flame sprayed to a stoichiometric composition, will be completely evaluated. Conventionally processed material calcined at higher temperatures will be evaluated. Also, further work will be directed towards learning more about flame sprayed-hot pressed materials. We will make a phase shifter using our best material. If the low field losses have not been eliminated, a suitable biasing d.c. voltage will be applied.

7. PROGRAM FOR THE NEXT INTERVAL

The work during the next interval will be primarily directed toward reducing or possibly eliminating low field loss and still retain a 200°C Curie point and satisfactory phase shift characteristics. Materials, which have been processed conventionally and flame sprayed to a stoichiometric composition, will be completely evaluated. Conventionally processed material calcined at higher temperatures will be evaluated. Also, further work will be directed towards learning more about flame sprayed-hot pressed materials. We will make a phase shifter using our best material. If the low field losses have not been eliminated, a suitable biasing d.c. voltage will be applied.

8. IDENTIFICATION OF PERSONNEL

Below is a list of the personnel working on this contract and the hours spent. The time has been recorded as to the amount supported by Airtron and the Government.

Hours Spent on Ferrite Development Contract

January 18, 1963, to April 18, 1963

Name	Airtron	Government
E. Anderson		1.0
A. Bates		91.0
R. Connolly		46.5
A. Dort		18.1
J. Horbacz		5.0
B. Kaplan	444.5	
K. Lehman		251.0
D. Lepore		317.0
J. Nielsen		81.0
M. Pashywak	180.0	
F. Stallone	44.95	
J. Zneimer		192.0
Total	677.45	1002.6

9. PROJECT PERFORMANCE AND SCHEDULE CHART

Figure 26 is the Project Performance and Schedule Chart.

PROJECT PERFORMANCE AND SCHEDULE

CONTRACT NO. Nobsr 87488 (REPORT) DATE: May 20, 1963

Period Covering 1-18-63 to 4-18-63

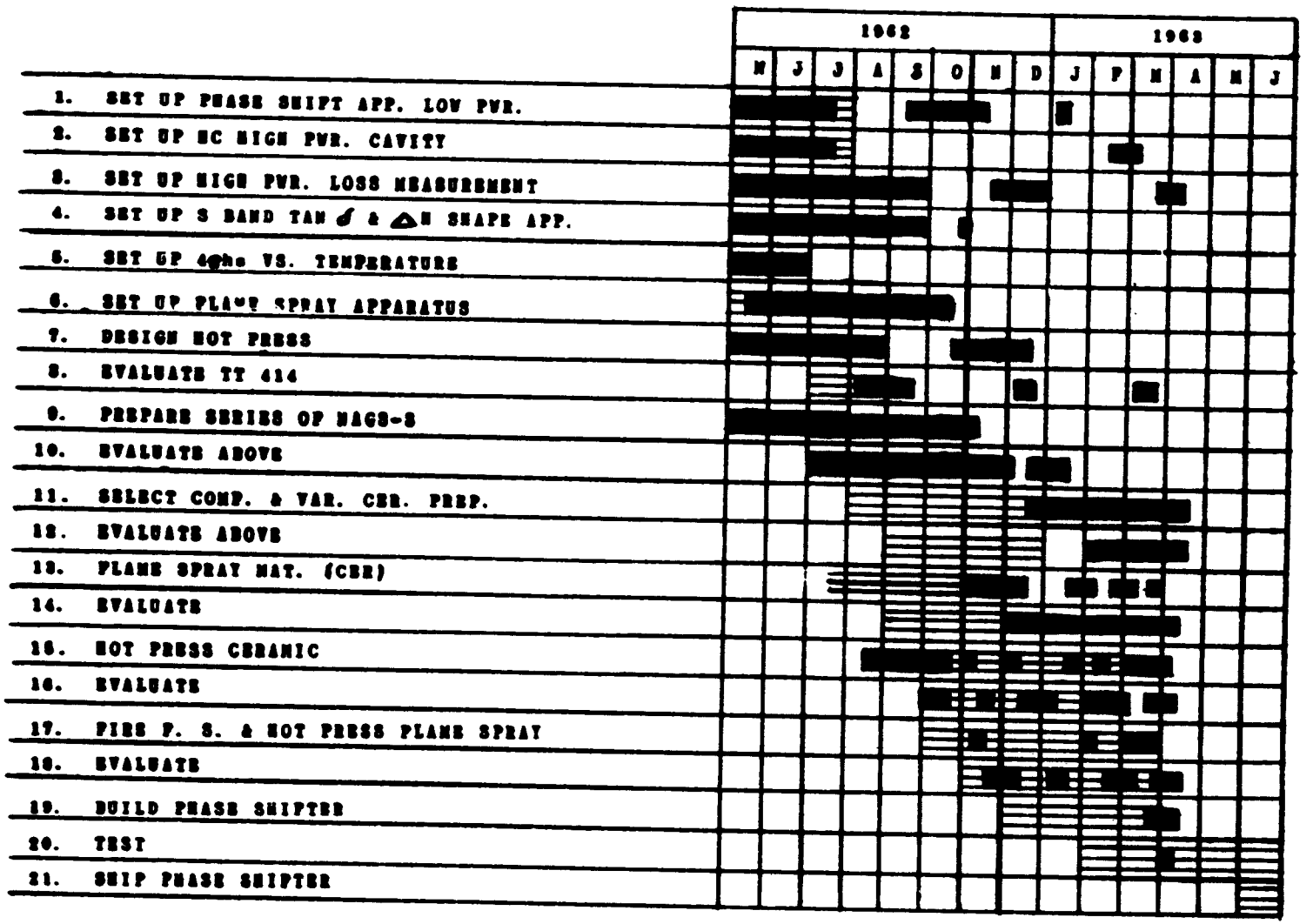

FIGURE 26 PROJECT PERFORMANCE AND SCHEDULE CHART

10. REFERENCES

1. E. G. Spencer and R. C. Le Craw, "Wall Effects on Microwave Measurements of Ferrite Spheres", J. App. Phys., 26, 250 (1955).

2. J. O. Artman and P. E. Tannenwald, "Measurement of Susceptibility Tensor in Ferrites", J. App. Phys., 26, 1124 (1955).

DISTRIBUTION LIST

	No. Copies
Advisory Group on Electron Devices 346 Broadway, 8th Floor New York 13, New York	3
Armed Services Technical Information Agency Arlington Hall Station Arlington 12, Virginia	10
Commanding Officer U. S. Army Electronics Research and Development Laboratory Attention: SELRA/SL-PEM (Dr. I. Bady) Fort Monmouth, New Jersey	1
Commander Naval Ordnance Laboratory White Oak, Applied Physcis Department Room 1-285, Administration Building Attention: Dr. Louis R. Maxwell, Chief Silver Spring, Maryland	1
Commander Rome Air Development Center Attention: Mr. Joseph Brauer, RAOT Griffiss Air Force Base, New York	1
Commander Air Force Cambridge Research Laboratory Bedford, Massachusetts Attention: Dr. Carl Pithia	1
Commander Aeronautical Systems Division Wright-Patterson Air Force Base, Ohio Attention: Mr. J. I. Wittebort	1
Director U. S. Naval Research Laboratory Attention: Dr. M. Kales, Code 5250 Washington 25, D. C.	1
Trans Tech Incorporated Gaithersburg, Maryland	1

DISTRIBUTION LIST

	No. Copies
Director U. S. Naval Research Laboratory Attention: Mr. J. Murray, Code 6430 Washington 25, D. C.	1
Bureau of Ships Code 335 Washington 25, D. C.	3
National Bureau of Standards Boulder Laboratories Boulder, Colorado Attention: Mr. J. L. Dalke	1
Bureau of Ships Code 681A2A Washington 25, D. C.	5
Inspector of Naval Material Route 22 Mountainside, New Jersey Attention: Mr. W. Ferfort	1